

Large Language Models: A Mathematical Formulation

Ricardo Baptista^{1,2}, Andrew Stuart^{3,4}, and Son Tran³

¹*Statistical Sciences, University of Toronto, Toronto M5G 1X6, Canada*

²*Vector Institute, Toronto, M5G 0C6, Canada*

³*Amazon Search, Palo Alto, CA 94301, USA*

⁴*Computing and Mathematical Sciences, California Institute of Technology, Pasadena CA 91125, USA*

r.baptista@utoronto.ca, andrxstu@amazon.com, sontran@amazon.com

Abstract: Large language models (LLMs) process and predict sequences containing text to answer questions, and address tasks including document summarization, providing recommendations, writing software and solving quantitative problems. We provide a mathematical framework for LLMs by describing the encoding of text sequences into sequences of tokens, defining the architecture for next-token prediction models, explaining how these models are learned from data, and demonstrating how they are deployed to address a variety of tasks. The mathematical sophistication required to understand this material is not high, and relies on straightforward ideas from information theory, probability and optimization. Nonetheless, the combination of ideas resting on these different components from the mathematical sciences yields a complex algorithmic structure; and this algorithmic structure has demonstrated remarkable empirical successes. The mathematical framework established here provides a platform from which it is possible to formulate and address questions concerning the accuracy, efficiency and robustness of the algorithms that constitute LLMs. The framework also suggests directions for development of modified and new methodologies.

Keywords and phrases: Language Models, Tokenization, Transformer Architecture, Self-attention, Maps on Measures, Probabilistic Prediction.

MSC2020 subject classifications: 65C20, 65K10, 68T01.

1. Introduction

1.1. Goal and Organization of Paper

Large language models (LLMs) have, in only a few years, revolutionized the field of artificial intelligence (AI). Their impact is being felt across society: they can help with tasks as diverse as the writing of computer code and the planning of a vacation itinerary; they can hold conversations; they can process medical information and ask follow-up questions to gather more information and provide potential diagnoses; they can retrieve and summarize information from different sources including legal documents and scientific papers; and they can interact with other sources of information such as images, audio and video. Their potential to permanently change our way of life is clear.

Yet the methodology, however impressive, is prone to errors, is not equipped with any rigorous logical or inferential constraints, comes with limited guarantees and consumes enormous resources, both to create and to deploy. This situation presents, then, as an opportunity for mathematicians to help to address these shortcomings by developing, and then studying, utilizing and evolving, a fundamental picture of how LLMs work. It is, however, not easy to find a complete presentation of how LLMs work, aimed at a mathematically inclined audience. This is because published work in the AI community relies primarily on communication through a combination of high-level visual sketches of AI algorithms, made precise through supporting code which is publicly available through, for

example, Github. This admirable approach to open-source software that produces published results has been central to the success of AI [31]; it has also revolutionized other fields, such as computational science and engineering, which now strive to meet the same standards of reproducibility as the AI community. However, the reliance on published code to precisely define the methodology underlying LLMs makes it difficult to formulate and address conceptual questions whose study might help to address the aforementioned shortcomings of LLMs. The goal of this paper is to present a precise mathematical formulation of LLMs; in doing so we aim to make the subject of LLMs accessible to mathematicians, and to provide a framework for subsequent computational and theoretical studies of LLMs by mathematicians.

The objects that are manipulated in LLMs are sequences; Section 2 sets up the notation that we employ for sequences, and describes different representations of language, as sequences of *tokens* and sequences in Euclidean space, that are relevant to the formulation of LLMs. In Section 3 we describe the core methodology by which LLMs work: *autoregressive factorization* of the probabilistic model for sequences, and *next-token prediction*; this includes a high-level description of the parameterization of models used for next-token prediction. Section 4 then describes the probabilistic objective function used in the training of these models, and the use of large corpora of data taken from the internet to define this objective. In Section 5 we detail the parameterization of models for next-token prediction, introducing the concepts of *positional encoding*, the *attention mechanism* and the *set transformer*; we also discuss the computational complexity of these parameterizations, and describe modifications, such as using *state-space models* in place of the attention mechanism, which have proven efficient in certain specific scenarios. Section 6 discusses different ways in which the next-token prediction model is used for *sequence generation*. In Section 7 we study various applications of these LLMs based on autoregressive factorization. Section 8 presents a framework to evaluate LLM’s sequence generation capabilities on various tasks. In Section 9 we describe an alternative emerging approach to autoregressive LLMs: generalization of diffusion-based generative modeling to discrete sequence space. Section 10 contains our concluding summary and discussion of challenges.

The Appendices contain mathematical details that are of interest, but which would break the flow if contained in the main body of the paper. Section A provides details of derivatives of the model, with respect to parameters to be learned; these derivatives are required to employ gradient descent-based methods in the training of LLMs. Section B provides a probabilistic perspective on the attention architecture; this perspective is of value when considering the use of the attention mechanism beyond the confines of LLMs. In Section C we describe a continuous time perspective on state-space models. This perspective underpins the original development of the methodology as a replacement for the attention mechanism; it is also useful when considering applications beyond the confines of LLMs. In Section D we present a proof on the reversibility of discrete diffusions; this underlies the sequence generation methodology described in Section 9. Section E contains additional details and responses from LLMs for the applications presented in Section 7.

1.2. Literature Review

Recent developments in LLMs are based on both theoretical foundations, and algorithmic innovations. It is argued persuasively in [31], that the impressive empirical success of LLMs is founded on their access to vast amounts of data, benchmarks agreed across the community and the sharing of computer code aimed at testing against these benchmarks. The resulting empirical studies have driven innovation resulting in popular commercial models such as LLaMa [95], GPT [2], Gemini [91], and Claude [7]; we refer to a recent survey of this field in [114]. LLMs as a tool for mathematicians have been reviewed in [35].

The first core ingredient of LLMs is the *transformer* architecture. This method for processing sequential data was first introduced in [97]. Transformers are studied from a mathematical perspective in [96]; and properties of the transformer architecture are analyzed in detail in [40, 24, 41, 20]. The transformer is based on the *attention mechanism*, a mapping that takes sequences into sequences. When the parameters defining the mechanism are suitably tuned to the data, the mapping can be used to learn about correlations between different elements in the input sequence. Attention is formulated mathematically in [16] and analyzed in detail in [39, 38, 57, 16]. In addition to their use in natural language processing, transformer architectures have been applied in other contexts including computer vision [32], time-series analysis and forecasting [6], nonlinear filtering [11], protein folding [55] and sequential decision making [23]. LLMs have also been tuned to improve their reasoning abilities to solve mathematical problems in [82]. We refer to [70] for the construction of many formal algorithms based on the transformer architecture. Several algorithmic variants on transformers have also been introduced to improve their efficiency for long sequences; these include approaches to reduce the quadratic complexity of standard self-attention [26, 29, 25, 92]. Other steps in transformers, such as normalization for training stability—typically achieved using a process known as layer normalization [10, 110]—have also been analyzed and explored through various methodological approaches [105, 116].

A second ingredient is *tokenization*. This has two key components: the introduction of a larger vocabulary of *tokens* in the service of shortening sequence length; and the identification of elements in this vocabulary of tokens with points in Euclidean space. The first component is typically achieved through *byte-pair encoding*, which was introduced as a method of file compression in [36], and appeared as an algorithm in the context of sequences in [119]. Byte-pair encoding assigns a new vocabulary element to frequently occurring adjacent pairs of vocabulary elements, and then applies this idea recursively. The method is modified for language modeling in [80] by adapting the algorithm to merge characters and produce a finite vocabulary of subword, and word, units, known as *tokens*. Machine translation techniques and transformers process these tokens to model language. Extensions to continuous token spaces with an infinite vocabulary have also been proposed [112]. Much of the text used in training LLMs is longer than the context window length used to take text as input. Decomposition of such larger text sequences, and merging them, so that the new units of text fit into the context window, can be done in multiple ways; optimizing for issues like memory allocation and information content is important in the decomposition process [30]. The second component, identifying each token with a point in Euclidean space, is undertaken as part of the training of the LLM architecture.

After training, the aim of LLMs is to generate text responses given starting prompts or questions, typically outside of the sequences seen during training. This process is performed using a deterministic or stochastic *decoding* procedure, that sequentially generates the tokens, from first to last, conditioned on preceding tokens. This concept of building a model to predict the next most likely word given the context of a sequence of words first originated in work by Shannon [81]. Several variants have been proposed to improve the correctness of the responses and avoid *hallucination*, whereby the model produces factually incorrect or inconsistent content, despite being readable. To improve the coherence and variety of generated text, top-k sampling was introduced in [48]. In the context of LLMs, *chain-of-thought reasoning* refers to models which generate responses explicitly outlining the reasoning process behind them. Recently, eliciting chain-of-thought reasoning by adapting the prompt [103] or changing the sampling strategy [102, 101] has been found to yield more factual responses in some settings.

In addition to sequential processing of sequences based on autoregressive decoding, other architectures have been proposed for text understanding and generation. These include BERT [103], which learns to unmask an arbitrary subset of elements of a sequence based on the surrounding context,

which is not necessarily contiguous in the sequence. Discrete diffusion models are an alternative procedure to generate an entire block of text using a time-dependent denoising process rather than sequentially generating each subsequent element of a sequence. Discrete diffusion models for finite state-space sequence generation were presented in discrete time in [49, 8] and extended to a continuous-time setting in [17]. Several choices for the noising process and objective functions have been proposed to learn the denoiser based on a discrete analog of score matching [63, 83, 79] and variational inference [89]. These methods currently achieve competitive performance to GPT-2 scale autoregressive models, but do not yet outperform more recent versions of GPT and similar commercial models.

Lastly, the autoregressive approach to text sequence generation has been extended to processing and generation of other data types, often referred to as multimodal LLMs. This data includes audio, images, and video, and can be continuous, semi-continuous or discrete. Common approaches [64, 104, 109] embed all data types into the embedding space for a language model and use autoregressive decoding and prediction to process and generate text or data from other modalities.

2. Sequences

This section is foundational in relation to the question of how language is represented in, and manipulated by, algorithms rooted in (floating point approximation of) Euclidean space. We start in Subsection 2.1 by establishing notation for finite sequences, over two *vocabularies* (finite sets), denoted V_0 and V , and over the Euclidean space \mathbb{R}^{d_e} . The discrete set V_0 defines the initial vocabulary used to describe inputs. The discrete set V defines a second vocabulary, defined from V_0 by a process known as byte-pair encoding, described in Subsection 2.2; this process results in a set V satisfying $|V| \gg |V_0|$. There is a bijection between sequences taking values in V_0 and in V . With respect to the pairing implied by this bijection the sequence taking values in V will be much shorter than the sequence taking values in V_0 , reflecting a natural trade-off between size of the alphabet and length of the sequence. In Subsection 2.3 we describe how each element in V is identified with a point in \mathbb{R}^{d_e} . This identification is a crucial step as it allows for *interpolation* in the space of text; the interpolation is performed in the Euclidean representation of the text sequence.

2.1. Notation for Sequences

A central component in our framing of LLMs is the manipulation of sequences defined over the finite integer set $S^M = \{1, \dots, M\}$ for various M . We will consider three types of sequences: the first where each element takes value in finite discrete set V_0 , the second where each element takes value in finite discrete set V , and the third where each element takes value \mathbb{R}^{d_e} . We write

$$F_0^M := \{f : S^M \rightarrow V_0\}, \quad F^M = \{f : S^M \rightarrow V\}, \quad F_o^M = \{f : S^M \rightarrow \mathbb{R}^{d_e}\}.$$

For $f \in F^M$ we sometimes write $f_{1:M}$ to emphasize the domain of the sequence; and we write $f_m \in V$ for the m^{th} entry of the sequence. Similar notation extends naturally to F_0^M and F_o^M .¹ We adopt the convention that $f_{1:0} = \emptyset$. A commonly occurring real-valued sequence will be an element of F_e^M , where \mathbb{R}^{d_e} is an *embedding space*. Finally we define $S^{M,M} := S^M \times S^M$.

2.2. Tokenization and Byte-Pair Encoding

Consider an initial vocabulary V_0 used to define input text as an element of $F_0^{M_0}$. The goal of *compression* is to reduce the length of an input sequence by identifying a new, much larger, vocabulary

¹Note the difference between number 0 (zero) and the letter o (denoting a generic lower case letter).

V , containing the initial vocabulary, and representing the text as an element in F^M for some M , typically much smaller than M_0 . Compression can be achieved by creating a vocabulary V from V_0 which is based on frequently-occurring strings of characters in V_0 . The vocabulary elements that result from this process are known as *tokens*. Currently *byte-pair encoding* [36] is widely used for tokenization in LLMs [76]; we explain this approach to encoding by means of examples.

Example 2.1. Consider a simple example of compression, starting with initial alphabet $V_0 = \{a, b, c\}$. Given the input sequence $f^{(0)} = \{abcababc\}$, the first iteration counts the occurrences of each pair of neighboring elements. The most frequently occurring pair is identified, in this case ab , and then labeled $d = ab$; it is then added to the vocabulary and $V_1 := V_0 \cup d$ is defined. In this new vocabulary, the input sequence is represented as $f^{(1)} = \{dcddc\}$. The idea of creating new vocabulary elements based on frequently occurring pairs is now recursed on. The second iteration identifies the element dc to be the most frequently occurring pair, defines the new element $e = dc$ and adds it to the vocabulary, defining $V_2 := V_1 \cup e$. The sequence is now represented as $f^{(2)} = \{ede\}$. This sequence cannot be compressed further using the notion of most frequently occurring neighbouring pairs. We thus define the final new vocabulary to be $V := V_2 = \{a, b, c, d, e\}$. In practice, this iterative procedure can also be stopped early after a pre-defined number of levels of recursion; in this simple example the algorithm might be stopped after one level and then choose $V := V_1 = \{a, b, c, d\}$, for instance, rather than after the two levels which lead to termination.

Example 2.2. Consider application of byte-pair encoding to an initial vocabulary V_0 defined by the English language; this will contain the standard lower case alphabet $\{a, b, \dots, y, z\}$, its upper-case version, as well as elements representing punctuation, spaces, new paragraph, start of text, end of text and the like; it may also contain symbols from computer code and include other alphabets, such as the Greek alphabet $\{\alpha, \beta, \dots, \omega\}$. Then $|V_0| = \mathcal{O}(10^2)$. Use of byte-pair encoding, based on studying frequencies in large text corpuses from the internet, leads to $|V| = \mathcal{O}(10^4)$ [73]. English language text of length several paragraphs can be represented as a sequence of length $M = \mathcal{O}(10^2)$ in the encoded vocabulary [53].

From now on we set $V := \{1, \dots, |V|\}$ noting that we may use this set of integer labels for the elements of V without loss of generality. Thus $V \equiv S^{|V|}$.

Example 2.3 (Example 2.1 continued). We have $V = \{a, b, c, d, e\}$. However without loss of generality we may relabel these elements as $V = \{1, 2, 3, 4, 5\}$.

Remark 2.4. When byte-pair encoding is used and recursed to significant depth. most commonly occurring words end up being represented by a single token.

Remark 2.5. Whilst byte-pair encoding has proven to be successful empirically, it is conceivable that other encodings might be desirable in some settings. In particular the trade-off between sequence length and vocabulary size may play out differently, in different tasks or on different architectures, in terms of associated computational cost for training and evaluation.

2.3. Making Language Euclidean

We now discuss how byte-pair encoded sequences in F^M can be represented as sequences in Euclidean space, that is as elements in F_e^M . This is done by assigning a unique element in \mathbb{R}^{d_e} to each point in V ; and indeed this assignation is typically learned as part of the training of the LLM from data. In this subsection the goal is to set-up a notation for this assignation process. The basic building block is the following definition of function $\phi : V \rightarrow \mathbb{R}^{d_e}$. Recall that $V = \{1, \dots, |V|\} = S^{|V|}$.

Definition 2.6. Let $\varphi \in \mathbb{R}^{d_e \times |\mathcal{V}|}$ be a matrix, where $\varphi = (\varphi_1, \dots, \varphi_{|\mathcal{V}|})$; here $\varphi_v \in \mathbb{R}^{d_e} \forall v \in \mathcal{V}$. Then, define $\phi : \mathcal{V} \rightarrow \mathbb{R}^{d_e}$ by $\phi(v) = \varphi_v \forall v \in \mathcal{V}$.

Given $f \in \mathsf{F}^M$ we extend ϕ to act on sequences:

Definition 2.7. Define $\phi : \mathsf{F}^M \rightarrow \mathsf{F}_e^M$ by $(\phi \circ f)_m = \phi(f_m)$.

Remark 2.8. The construction of ϕ to act on sequences in F^M is parameterized by φ . The parameterization is independent of sequence length M . This is because ϕ is defined to act elementwise on the sequence. We will see later that the other learnable parameters in LLMs are also defined in a manner which is independent of sequence length. This is an important feature of the parameterization of LLMs as it enables a common model to be deployed to manipulate sequences of different lengths.

Remark 2.9. It is natural to ask whether φ could be defined, or learned, independently of LLM training. In particular there is nothing in the current learning of the embedding which ensures that, for example, two words which are synonymous with one another are close when embedded in Euclidean space; indeed two words which are synonymous may even be comprised of different numbers of tokens. For example, if one such word is used infrequently and is not represented as a single token, whilst the other is frequently used and is represented as a single token, then the two words are not even embedded in the same Euclidean space. Addressing this issue might involve moving beyond byte-pair encoding; see Remark 2.5.

2.4. Encoding Other Data Modalities

Here we discuss the representation of input modalities, other than text, as a sequence. This is the basis for *multimodal LLMs* which facilitate communication between different data modalities. We start by focusing on images. Given a bounded domain $D \subset \mathbb{Z}^2$, an image is given by a mapping $f : D \rightarrow \mathbb{R}^{d_c}$ where d_c is a channel dimension; this is taken to be $d_c = 1$ for grayscale images and $d_c = 3$ for RGB images. The domain D can be flattened into a set with $M = |D|$ elements that is indexed by a single parameter so that the image f can be represented in the space of sequences F_c^M . This is analogous to the space F_e^M for the Euclidean embedding of text sequences.

For text sequences it has been empirically observed that it is advantageous to shorten the length of sequences at the expense of a larger vocabulary. A similar trade-off is present for images, with channel width playing the role of vocabulary size. The next example illustrates this.

Example 2.10. The CLIP algorithm [71] is a contrastive learning approach [14] used in the alignment of text and images. It employs a methodology to process images as sequences that trades sequence length with channel width. To explain CLIP in a concrete context we assume that we are dealing with RGB images, and that $D = \mathbb{S}^{K', K'}$. Then the image can be viewed as $i_{\text{original}} : \mathbb{S}^{K', K'} \rightarrow \mathbb{R}^3$. By application of a linear convolution operator this is mapped to $i_{\text{convolved}} : \mathbb{S}^{K, K} \rightarrow \mathbb{R}^{d_l}$. This is then flattened to obtain $i_{\text{sequence}} : \mathbb{S}^{K^2} \rightarrow \mathbb{R}^{d_l}$. If d_l coincides with the text embedding dimension d_e then the resulting sequence is indeed in F_e^M . In CLIP, the specific values used for the dimensions are $K' = 224$, $K = 7$ and $d_l = 768$; furthermore d_l is indeed chosen to coincide with the text embedding dimension d_e . Noting that $768 \gg 3$ and that $K^2 \ll (K')^2$ we see that, as with text, we have again shortened the length of the sequence at the expense of increasing some measure of the size of the space in which each element of the sequence lies.

Remark 2.11. For 8-bit RGB images, the intensity of given colour at each pixel is often given by an integer between 0 and 255 rather than an arbitrary real number. Hence, images can also be represented as mappings with discrete outputs, i.e., $i_{\text{original}} : \mathbb{S}^{K', K'} \rightarrow \{0, \dots, 255\}^3$, which corresponds to a tensor of integers of size $K' \times K' \times 3$. However, in practice these images are treated as having

continuous outputs, which become the inputs to neural network-based vision encoders; see Section 7.7 for more details on the encoding process.

Other frequently occurring modalities include audio and video. Audio, similarly to text, is best thought of as a sequential time-series. In many circumstances this sequences takes values in Euclidean space; but, as discussed in Remark 2.11 in the setting of RGB images, this information is often discretized and represented in a set of integers. Video is processed by treating the data as a sequence of images, also known as frames. Hence, for $D = \mathbb{S}^{K', K'}$, a video can be described by a space-time mapping $f: [0, T] \times D \rightarrow \mathbb{R}^{d_v}$ for some final time T . In practice, the time-domain is discretized based on the frequency of image capture, known as the frame rate. For example, a video can be discretized into a finite number D_T of frames; this results in a mapping from $D_T \times D$ to \mathbb{R}^{d_v} . To reduce the memory required to store a video and reduce redundant information across frames, it is often necessary to further sub-select frames, which are not necessarily equally spaced in time; see [51] for a recent approach to frame selection. Finally we note that video and audio are often coupled, through a common time-indexing to create audio-visual data. Multimodal LLMs are being developed to co-process text, image, audio, video and audio-visual data.

3. Next-Token Prediction

Next-token prediction is central to LLMs. For a sequence of length m , $f_{1:m} \in \mathbb{F}^M$, next-token prediction works by assigning probabilities of token f_m taking values at each element in $\mathbb{V} = \mathbb{S}^{|\mathbb{V}|}$, conditional on the entire preceding sequence $f_{1:m-1} \in \mathbb{F}^{M-1}$ of tokens. Throughout this section we use $\mathcal{P}(\cdot)$ to denote a probability space, either over \mathbb{V} and denoted $\mathcal{P}(\mathbb{V})$, or over sequences of arbitrary length M , where each element takes values in \mathbb{V} , and denoted $\mathcal{P}(\mathbb{F}^M)$. The starting point of next-token prediction is a probability model for sequences $f_{1:\ell} \in \mathbb{F}^\ell$, for $\ell = 1, \dots, L$, where L denotes a pre-specified maximum *context length* L .²

In Subsections 3.1 we describe *autoregressive* factorizations of probability distributions on sequences; this factorization builds in the idea of next-token prediction into the factorization. Then in Subsection 3.2 we describe the form of approximations we use for this autoregressive factorization. Recall from Definition 2.7 that application of ϕ to $f_{1:m-1} \in \mathbb{F}^{m-1}$ embeds the sequence $h_{1:m-1}$ in Euclidean space \mathbb{F}_e^{m-1} . In order to take advantage of advances in neural networks and related architectures for classification defined for inputs in Euclidean space, we make use of approximation architectures that take as input the sequence $h_{1:m-1} := \phi \circ f_{1:m-1} \in \mathbb{F}_e^{m-1}$.

3.1. Autoregressive Factorization Of Probability Distributions On Sequences

The heart of next-token prediction is the *auto-regressive factorization* of $\mathbf{p}_{1:L} \in \mathcal{P}(\mathbb{F}^L)$ given by

$$\mathbf{p}_{1:L}(f_{1:L}) = \prod_{\ell=1}^L \mathbf{p}_\ell(f_\ell | f_{1:\ell-1}). \quad (3.1)$$

We will also need the analogous autoregressive factorization of $\mathbf{p}_{1:\ell} \in \mathcal{P}(\mathbb{F}^\ell)$ for subsets of sequences of any length $\ell \in \mathbb{S}^L$:

$$\mathbf{p}_{1:\ell}(f_{1:\ell}) = \prod_{m=1}^\ell \mathbf{p}_m(f_m | f_{1:m-1}). \quad (3.2)$$

Here, for each input sequence $f_{1:m-1} \in \mathbb{F}^{(m-1)}$, $\mathbf{p}_m(\cdot | f_{1:m-1}) \in \mathcal{P}(\mathbb{V})$. Alternatively we may write $\mathbf{p}_m(\cdot | \cdot) : \mathbb{F}_e^{(m-1)} \rightarrow \mathcal{P}(\mathbb{V})$. We refer to $\mathbf{p}_m(\cdot | f_{1:m-1}) \in \mathcal{P}(\mathbb{V})$ as the *target next-token probability* at position m in the text sequence, noting that it is a conditional probability of token at index m , given the sequence $f_{1:m-1}$ of tokens seen up to $m-1$.

²Sometimes also known as the *context window*.

Remark 3.1. The discrete probability distribution on $\mathbf{p}_{1:\ell} \in \mathcal{P}(\mathbf{F}^\ell)$, any $\ell = 1, \dots, L$, or on $\mathbf{p}_\ell(f_\ell | f_{1:\ell-1}) \in \mathcal{P}(\mathbf{V})$, any $\ell = 1, \dots, L$, should be thought of as being defined empirically by the set of all text available on the Earth at this moment in time, either on the internet or in hard-copy documents. In practice an approximation is learned through accessing a (vast) subset of such data from the internet. More information on the training data is provided in Remarks 4.2 and 4.3.

LLMs work by *rolling out* sequences in \mathbf{V} step-by-step, starting with a sequence of a given length, then increasing the sequence length by one in steps until it reaches length L . The main part of this process is to take a sequence of length $m-1$ and predict the probability, for each token in \mathbf{V} , of occupying the m^{th} entry of the sequence. The probabilistic structure can be used to roll-out sequences in various different ways, which we describe in detail in Section 6.

Example 3.2 (Example 2.2 continued). All production LLMs have a maximum number of tokens that are processed at once. For instance, the popular LLaMA-2 7 billion model has a context window of $L = 4096$ tokens [95]³. This length corresponds, in a byte-pair encoded alphabet, to up to several pages of text. The CLIP model for alignment of (for example) text and images uses $L = 77$, corresponding, in a byte-pair encoded alphabet, to up to several paragraphs of text [71]. Linking to Example 2.2 demonstrates the trade-off being made here between vocabulary size and sequence length. Both have implications for computational efficiency: the attention-based architectures, described in detail in Section 5, have cost which scales quadratically in sequence length, to evaluate; on the other hand the size of vocabulary has impact on memory requirements and on the training problem defined in Section 4. Understanding how to optimize this trade-off between sequence length and vocabulary size remains an open question.

3.2. Approximation Of Probability Distributions On Sequences

We seek a θ -parameterized family $\pi_{1:L}(f_{1:L}; \theta)$ from which to find an approximation of $\mathbf{p}_{1:\ell}(f_{1:\ell})$ given in (3.1). Here $\theta \in \Theta \subseteq \mathbb{R}^p$. Motivated by (3.1) we also seek the approximation family in autoregressive form:

$$\pi_{1:L}(f_{1:L}; \theta) = \prod_{\ell=1}^L \pi_\ell(f_\ell | f_{1:\ell-1}; \theta), \quad (3.3)$$

for $\theta \in \Theta \subseteq \mathbb{R}^p$. We thus wish to approximate, for each m , the next-token conditional probability $\mathbf{p}_m(\cdot | f_{1:m-1})$ by a model distribution $\pi_m(\cdot | f_{1:m-1}; \theta) \in \mathcal{P}(\mathbf{V})$ for each conditioning sequence of length $m-1$ and choice of parameter $\theta \in \Theta$. The parameterization of this function by sequence $f_{1:m-1} \in \mathbf{F}^{(m-1)}$ makes learning from data difficult, because \mathbf{V} , and hence $\mathbf{F}^{(m-1)}$, is a discrete space with no notion of continuity. Thus we seek to embed \mathbf{V} in Euclidean space \mathbb{R}^{d_e} for some embedding dimension d_e . To do this we use the map ϕ from Definition 2.6, and its extension to sequences from Definition 2.7. We recall that ϕ is defined by matrix $\varphi \in \mathbb{R}^{d_e \times |\mathbf{V}|} \cong \mathbb{R}^{p_e}$, and define $\theta = (\vartheta, \varphi)$ for parameter $\vartheta \in \mathbb{R}^{p_a}$. Then $\theta \in \mathbb{R}^p$, where $p = p_a + p_e$ and $p_e = d_e |\mathbf{V}|$. We then seek to parameterize π_m in the form

$$\pi_m(f_m | f_{1:m-1}; \theta) := \mathbf{q}_m(f_m | \phi \circ f_{1:m-1}; \vartheta). \quad (3.4)$$

Thus, for fixed ϑ , $\mathbf{q}_m(\cdot | \cdot; \vartheta) : \mathbf{F}_e^{(m-1)} \rightarrow \mathcal{P}(\mathbf{V})$. For each m , learning π_m in this form reduces to learning a map from $\mathbf{F}_e^{(m-1)}$, sequences in \mathbb{R}^{d_e} of length $(m-1)$, into the probability simplex $\mathcal{P}(\mathbf{V})$.

Example 3.3. Learning a map from \mathbb{R}^d to a probability simplex on a finite set is a standard machine learning problem, known as classification. It is at the core of the solution of the digit labeling problem addressed on the MNIST data set in the seminal paper [60]. In that context $d = 28^2$ and the cardinality of the set underlying the probability simplex is 10.

³Recent LLaMA models with more parameters and specialized fine-tuning support up to $L = 128K$ tokens [44]

In the context of language models we are learning “classifiers” from Euclidean spaces of dimension $(m - 1)d_e$, for $m = 1, \dots, L$ into a set of cardinality $|\mathcal{V}|$; in the case of byte-pair encoding of the internet corpora; recall from Example 2.2 that $|\mathcal{V}| = \mathcal{O}(10^4)$. Despite being a familiar problem, analogous to classification, it is rendered complex here for several reasons: (i) we have sought to parameterize \mathbf{q}_m by the *same* parameter θ , independently of m —thus we are seeking a single classifier that works on input sequences of arbitrary lengths; and (ii) this choice of parameterization couples together the \mathbf{q}_m for all $m = 1, \dots, L$, giving the parameter learning problem (discussed in detail in the next section) access to a large volume of data: it is necessary to consider multiple sequences of all lengths $m = 1, \dots, L$ simultaneously; and finally (iii) the number of labels $|\mathcal{V}|$ is large, of $\mathcal{O}(10^4)$.

4. Training Of The LLM

In this section we present the learning problem for the optimal choice of parameter $\theta \in \Theta \subseteq \mathbb{R}^p$ required to define the approximate next-token probability model described in Subsection 3.2. We denote this optimal choice by θ^* . We have explained that this parameterization couples together the learning at different sequence lengths. It is intuitive that this will create better next-token prediction; but it also leads to a substantial computational task, one which we now detail. The learning of the model is undertaken on the basis of the following data assumption.

Data Assumption 4.1. *We collect samples of i.i.d. sequences $\{f_{1:L}^{(n)}\}_{n=1}^N \sim \mathbf{p}_{1:L}$.*

The objective that is minimized to determine θ is formulated as minimizing a divergence between the data distribution, written in the form (3.1), and the proposed θ —dependent model distribution, determined by (3.3), (3.4). We introduce the population-level objective function and learning problem in Subsection 4.1; and then an empirical objective function, which is implemented in practice, in Subsection 4.2. Using the autoregressive structures (3.1) and (3.3) we derive a decompositions of the original objective. The original objective is defined over the joint distribution defined by the entire sequence of length L ; this is decomposed into a sum of coupled objectives each of which matches the conditional distribution on the next-token, given the preceding sequence, for all sequences of lengths up to $L - 1$. This decomposition reveals that the proposed objective strives to ensure that the model is accurate when conditioning on sequences of arbitrary length.

Before defining population and empirical optimization problems, we recall the Kullback-Leibler (KL) divergence between probability distributions \mathbf{p}, \mathbf{p}' defined over the same space and with common support:

$$D_{KL}(\mathbf{p} || \mathbf{p}') = \mathbb{E}_{f \sim \mathbf{p}} \left[\log \frac{\mathbf{p}(f)}{\mathbf{p}'(f)} \right]. \quad (4.1)$$

Use of this divergence as the basis for definition of objective functions leads to the decompositional structure alluded to in the previous paragraph. In the following sections we demonstrate this fact, and highlight a practical optimization problem for θ that may be implemented as a result. Before this, we make two remarks about the data employed in training.

Remark 4.2 (Remark 3.1 continued). *We have defined probabilities $\mathbf{p}_{1:L}$ with respect to all text available on the Earth. But in practice an approximation is learned through accessing a (vast) subset of such data from the internet. So, although N is large, it is not the case that all data defining $\mathbf{p}_{1:L}$ is used. Many proprietary models do not report details of training data used, but some do. For example, the LLaMa-3 models were trained on a corpus of about 15 trillion multilingual tokens [44], increasing from the 2 trillion tokens used to train LLaMA-2 models [95]. The data used arises from several sources. For example, early GPT-3 models used a combination of data sources such as Common Crawl, books and the English Wikipedia pages [15]. With the increasing number of tokens used, and*

with current understanding about how much data is required, it is estimated that model training requirements will require the totality of all available human-generated text data on the web, which contains a median of 3100 trillion tokens, between 2026 and 2032 [98]. To address potential data scarcity, we note that more data is available in the form of images and videos. Furthermore recent models have also started to incorporate synthetic data for training [1]; the effect of synthetic data on model collapse is studied in [37].

Remark 4.3 (Data Processing). *The training data employed for several commercial models are determined by curating and filtering web data. This process includes removing harmful material, copyrighted content, duplicates and outliers. Furthermore, training algorithms are often run several times, with different balances of the constituent types of data (text, code, mathematical calculations and so forth) in order to improve the model’s performance on specific benchmarks. This can be helpful for tasks such as mathematical reasoning [15]. The processing increases the quality and diversity of samples, thereby reducing correlations between sequences. However, the processing results in shifts to the data distribution which are a function of the performance on the entire dataset. In practice, this violates having i.i.d. samples in Data Assumption 4.1.*

4.1. Population-Level Objective

The learning problem for the joint model over sequences of length L is now presented. Recall the true data distribution $\mathbf{p}_{1:L}$, from (3.1), our approximate distribution $\pi_{1:L}$, from (3.3), and the KL divergence (4.1). Using these constituents we define the following optimization problem:

Optimization Problem 4.4.

$$\begin{aligned} J(\theta) &:= D_{\text{KL}}(\mathbf{p}_{1:L} || \pi_{1:L}(\cdot; \theta)), \\ \theta^* &\in \arg \min_{\theta} J(\theta). \end{aligned}$$

This problem assumes access to the data distribution $\mathbf{p}_{1:L}$, leading to the population-level objective. The optimization problem is well-defined if $\mathbf{p}_{1:L}$ has density with respect to $\pi_{1:L}$, with both viewed as measures supported on \mathcal{F}^L . Solving this optimization problem is thus targeted at choosing the parameters $\theta = (\vartheta, \varphi)$ so that the approximate next-token prediction model (3.3) gives rise to sequences with similar distribution to those seen in the data distribution (3.1). The choice of KL divergence has two benefits: (i) as we show in this subsection, it naturally exploits the autoregressive structure that is integral to next-token prediction; (ii) as we show in the next subsection, the ordering of the two probability distributions within the KL divergence leads to an objective function which can be evaluated using only samples from $\mathbf{p}_{1:L}$ as detailed in Data Assumption 4.1.

We thus start by showing how to exploit structure in the objective function, using autoregressive factorization. From (3.1) and (3.3) we obtain

$$J(\theta) = \mathbb{E}_{f_{1:L} \sim \mathbf{p}_{1:L}} \left[\log \left(\frac{\mathbf{p}_{1:L}(f_{1:L})}{\pi_{1:L}(f_{1:L}; \theta)} \right) \right] \quad (4.2a)$$

$$= \sum_{\ell=1}^L \mathbb{E}_{f_{1:L} \sim \mathbf{p}_{1:L}} \left[\log \left(\frac{\mathbf{p}_{\ell}(f_{\ell} | f_{1:\ell-1})}{\pi_{\ell}(f_{\ell} | f_{1:\ell-1}; \theta)} \right) \right] \quad (4.2b)$$

$$= \sum_{\ell=1}^L \mathbb{E}_{f_{1:\ell} \sim \mathbf{p}_{1:\ell}} \left[\log \left(\frac{\mathbf{p}_{\ell}(f_{\ell} | f_{1:\ell-1})}{\pi_{\ell}(f_{\ell} | f_{1:\ell-1}; \theta)} \right) \right] \quad (4.2c)$$

$$= \text{const} - \sum_{\ell=1}^L \mathbb{E}_{f_{1:\ell} \sim p_{1:\ell}} \log \pi_\ell(f_\ell | f_{1:\ell-1}; \theta), \quad (4.2d)$$

where const indicates a scalar that does not depend on θ . We note that (4.2b) follows from imposing the autoregressive structure on (4.2a). Then (4.2c) follows because the input to the logarithm depends only on sequences of length ℓ . Finally we obtain (4.2d) since $p_\ell(f_\ell | f_{1:\ell-1})$ does not depend on θ . Given (4.2d), and the proposed model form in (3.4), it is thus natural to define the objective:

$$L(\theta) = - \sum_{\ell=1}^L \mathbb{E}_{f_{1:\ell} \sim p_{1:\ell}} \log \pi_\ell(f_\ell | f_{1:\ell-1}; \theta), \quad (4.3a)$$

$$= - \sum_{\ell=1}^L \mathbb{E}_{f_{1:\ell} \sim p_{1:\ell}} \log q_\ell(f_\ell | \phi \circ f_{1:\ell-1}; \vartheta). \quad (4.3b)$$

Since $J(\theta) = L(\theta) + \text{const}$ it follows that the minimizers of $J(\cdot)$ and $L(\cdot)$ coincide. Recall that form (4.3b) makes explicit that the model takes as input sequences in F_e^ℓ , allowing for the generalization properties of machine learning algorithms in Euclidean space to be exploited. Recall also that ϕ is defined by matrix φ and that $\theta = (\vartheta, \varphi)$.

Remark 4.5. *We note from (4.2c) that*

$$J(\theta) = \sum_{\ell=1}^L \mathbb{E}_{f_{1:\ell-1} \sim p_{1:\ell-1}} \mathbb{E}_{f_\ell \sim p_\ell(\cdot | f_{1:\ell-1})} \left[\log \left(\frac{p_\ell(f_\ell | f_{1:\ell-1})}{\pi_\ell(f_\ell | f_{1:\ell-1}; \theta)} \right) \right] \quad (4.4a)$$

$$= \sum_{\ell=1}^L \mathbb{E}_{f_{1:\ell-1} \sim p_{1:\ell-1}} D_{\text{KL}}(p_\ell(\cdot | f_{1:\ell-1}) || \pi_\ell(\cdot | f_{1:\ell-1}; \theta)). \quad (4.4b)$$

This shows that minimizing the objective function aims at choosing parameter θ so that next-token prediction accurately mimics next-token probabilities for conditioning sequences of all lengths up to $L-1$, on average; the fact that the same parameter θ appears for all sequence input lengths couples the different sequence lengths. Furthermore, since all terms in this sum are positive, it is apparent that had each conditional π_ℓ been parameterized independently by θ_ℓ , for different ℓ , then it would be possible to optimize each conditional alone. Moreover, the non-parametric minimizer of each term in the objective would be $\pi_\ell(\cdot | f_{1:\ell-1}; \theta_\ell^) = p_\ell(\cdot | f_{1:\ell-1})$.*

Remark 4.6. *The objective in Optimization Problem 4.4, defined through the KL divergence between sequences of length L , can also be defined in terms of any other choice of divergence D . However, in order for these divergences to be the basis of practical algorithms, it is necessary to be able to minimize this divergence without knowledge of the normalization constant of the target measure we are approximating, and given only samples from $p_{1:\ell}$ for all $\ell \in S^L$.*

Furthermore we note that use of $D = D_{\text{KL}}$ yields, using positivity of KL divergence and (4.4b), the inequality

$$D(p_{1:L} || \pi_{1:L}) \geq \mathbb{E}_{f_{1:m-1} \sim p_{1:m-1}(\cdot)} D(p_m(\cdot | f_{1:m-1}) || \pi_m(\cdot | f_{1:m-1})).$$

Thus making the left hand side small through minimization also ensures that the right-hand side is small, for any $m \in S^L$. This provides a quantitative estimate of the error in next-token prediction for any such m . On the assumption that next-token prediction is used to generate text, use of divergences other than KL will ideally share this, or similar, desirable property enabling the bounding of next-token probability prediction in terms of the objective on sequences of length L .

4.2. Empirical Objective

Recall parameter $\theta = (\vartheta, \varphi)$, where matrix φ defines the mapping ϕ between the tokenized and Euclidean representation of a given sequence, which is learned. We have identified $L(\theta)$ in (4.3b) as the function we wish to minimize. We have available to us data as prescribed in Data Assumption 4.1. Using this we can form the empirical measure that approximates $p_{1:\ell}$, for any $\ell \in \mathbb{S}^L$:

$$p_{1:\ell}^N := \frac{1}{N} \sum_{n=1}^N \delta_{f_{1:\ell}^{(n)}}.$$

Using this approximation in the objective function $L(\cdot)$ from (4.3b) we obtain the objective function minimized in practice:

$$L^N(\theta) = - \sum_{n=1}^N \sum_{\ell=1}^L \log q_\ell(f_\ell^{(n)} | \phi \circ f_{1:\ell-1}^{(n)}; \vartheta). \quad (4.5)$$

Remark 4.7. *An unbiased estimator for the objective function L in (4.3b) is given by drawing N i.i.d. sequences of length ℓ , and doing so independently for each $\ell = 1, \dots, L$. However, correlated samples can also be used: the empirical objective in (4.5) is defined by first drawing sequences of maximum length L and then using partial subsets of the same sequence to estimate the expectation for each ℓ .*

Learning the model parameters by minimizing (4.5) given text sequences from various domains is also known as *supervised pretraining*. The resulting next-token prediction model found this way is often referred to as a *pretrained model* or a *foundation model*. These models can be adapted for specific domains using fine-tuning or reinforcement learning, which we describe next.

4.3. Fine-Tuning The Empirical Objective

In the previous subsection, we describe the optimization of parameter $\theta = (\vartheta, \varphi)$, for the LLM through minimization of an empirical objective function (4.5) that is based on data reflecting the variety of tasks for which the LLM might be used. In the context of this subsection, we refer to this as *pretraining*. *Fine-tuning* with task-specific data is used to improve the performance of a pretrained model on a specialized class of tasks. The fine-tuned model is often found from an optimization problem identical to that defined by (4.5), but using a different (and typically much smaller) data set. The following assumption provides a setup for the fine-tuning data, which may be drawn from a distribution $p'_{1:L}$ that is different from the distribution $p_{1:L}$ used in pretraining. The distribution $p'_{1:L}$ will typically represent data for a specific task, but will ideally be close to $p_{1:L}$ after conditioning on a set related to the specific task defining the fine-tuning data.

Data Assumption 4.8. *We collect samples of i.i.d. sequences $\{f_{1:L}^{(n)}\}_{n=1}^{N_{\text{fine}}} \sim p'_{1:L}$.*

Using this data, the objective function minimized during the fine-tuning stage is given by:

$$L^{N_{\text{fine}}}(\theta) = - \sum_{n=1}^{N_{\text{fine}}} \sum_{\ell=1}^L \log q_\ell(f_\ell^{(n)} | \phi \circ f_{1:\ell-1}^{(n)}; \vartheta). \quad (4.6)$$

Algorithms for this fine-tuning optimization problem are typically initialized at the model parameters found from pretraining, thus connecting the information in the smaller, fine-tuning, data set to the larger data set used for pretraining. The resulting (approximate) minimizer is denoted by θ^{fine} .

Remark 4.9. The updates of the parameters during fine-tuning (e.g., neural network weights) are commonly restricted to be low-rank matrices using the widely-adopted Low-rank Adaptation (LoRA) procedure [50]. This restriction of the parameter changes improves computational efficiency by reducing the number of trainable parameters and results in an implicit form of regularization; see Section 4.5 for discussion of other regularization approaches employed during LLM training.

4.4. Reinforcement Learning

It is frequently the case that LLMs are modified to increase alignment of model responses with human preferences. This may be performed instead of, or in addition to, fine-tuning. Alignment to human preferences can be achieved using *reinforcement learning*. In this approach the model parameters are updated to maximize a reward function $\mathbf{r}: \mathcal{F}^L \rightarrow \mathbb{R}$ that approximates human preferences. In practice, the reward function is learned [27, 68, 118] or is defined implicitly by preference data [74]. A common framework is known as Reinforcement Learning from Human Feedback (RLHF) [87, 9]; this approach minimizes the negative reward while staying close to a reference model obtained from a pretraining or fine-tuning procedure as in subsections 4.2 and 4.3. The RLHF objective is given by:

$$\mathcal{L}^{\text{RL}}(\theta) = -\mathbb{E}_{f_{1:L} \sim \pi_{1:L}(\cdot; \theta)}[\mathbf{r}(f_{1:L})] + \beta \mathcal{D}_{\text{KL}}(\pi_{1:L}(\cdot; \theta) \parallel \pi_{1:L}(\cdot; \theta^{\text{ref}})); \quad (4.7)$$

here $\beta > 0$ is a tuning parameter and θ^{ref} refers to the minimizer of (4.5) or (4.6). This objective function is typically minimized starting from the reference model parameters θ^{ref} . In practice, the minimization problem is solved numerically by approximating the expectation over $\pi_{1:L}(\cdot; \theta)$, which is required in the definition of both terms, via sampling. Given a set of N_{RL} samples $f_{1:L}^{(n)} \sim \pi_{1:L}(\cdot; \theta)$, which depend on θ and thus are generated at each training iteration, the empirical objective function is given by:

$$\mathcal{L}^{\text{RL}, N}(\theta) = \frac{1}{N_{\text{RL}}} \sum_{n=1}^{N_{\text{RL}}} -\mathbf{r}(f_{1:L}^{(n)}) + \beta \log \left(\frac{\pi_{1:L}(f_{1:L}^{(n)}; \theta)}{\pi_{1:L}(f_{1:L}^{(n)}; \theta^{\text{ref}})} \right). \quad (4.8)$$

Remark 4.10. Pretraining and fine-tuning, defined in subsections 4.2 and 4.3 respectively, require samples from the data distributions as in Data Assumptions 4.1 and 4.8. Solving these optimization problems does not require generating sequences from the LLM during training. On the other hand, evaluating objective (4.7) in reinforcement learning does require sampling such sequences. This facilitates the calculation of the expected reward and the regularizing divergence. Given that the densities for both approximate distributions are analytically available, we can employ various divergences here, not just the reverse KL divergence used above.

4.5. Minimizing The Objective Functions

Approximate minimization of all of the objective functions (4.5), (4.6) and (4.8) is typically achieved using a stochastic gradient descent (SGD) procedure [78]. Currently deployed versions of the methodology, such as the widely used Adam optimization method [3], regularize to avoid overfitting to the data and to improve generalization: that is, to promote desirable model response in the generation of new sequences not present in the empirical dataset defined in Data Assumption 4.1; or, in the fine-tuning set-up, new sequences not present in the empirical dataset defined in Data Assumption 4.8. Common regularization methods applied during SGD include dropout [115, 108] and early stopping [56]. Sometimes L^2 regularization (often termed weight decay in the machine learning community), or other Tikhonov regularization [33] techniques, is applied directly to the objective function, rather than implicitly regularizing through the iterative optimization method [28, 59].

5. Architecture

In this section we detail the architecture enabling approximation of $\mathbf{p}_{1:L}$ from (3.1) by $\pi_{1:L}$ defined by (3.3), (3.4). We recall the form of the approximation here:

$$\pi_{1:L}(f_{1:L}; \theta) = \prod_{\ell=1}^L \pi_\ell(f_\ell | f_{1:\ell-1}; \theta), \quad (5.1a)$$

$$\pi_m(f_m | f_{1:m-1}; \theta) = \mathbf{q}_m(f_m | \phi \circ f_{1:m-1}; \vartheta). \quad (5.1b)$$

The parameter $\theta = (\vartheta, \varphi)$ is to be chosen to optimize the approximation. Through Definitions 2.6, 2.7 we have detailed the dependence on matrix φ which defines the mapping ϕ ; recall that this mapping enables \mathbf{q}_m to take sequences in *Euclidean space* as input, rather than the discrete *token space*, hence facilitating the possibility of *interpolation*. In particular, this interpolation allows the model to make next-token predictions for sequence that are not in the training data. In this section, we detail how the parameter ϑ enters (5.1b); then the value of the parameter θ is chosen to make the interpolation effective, via the training process described in Section 4.

To parameterize the model \mathbf{q}_m we will introduce the *set transformer*, which is based on the *attention mechanism*. Subsection 5.1 is a self-contained description of the attention mechanism; we introduce *attention maps*, families of parameterized maps acting on the space of Euclidean vector-valued sequences into itself, for sequences of any length. These attention maps are combined with *normalization maps* and *neural networks* to define the *attention block*. In Subsection 5.2 attention blocks are composed with one another, and with a final map into Euclidean space, to define the set transformer. The resulting map, parameterized by ϑ , takes as input Euclidean vector-valued sequences of arbitrary length and outputs elements in the probability simplex on \mathbf{V} . Subsection 5.3 describes refinements of, or alternatives to, the attention mechanism; the purpose is to incorporate more complex temporal structure, such as causality, and relatedly to reduce the complexity of the evaluation of the attention map.

5.1. The Attention Mechanism

We start by defining the *attention mechanism* $\text{ATT} : \mathbf{F}_e^{(m-1)} \rightarrow \mathbf{F}_e^{(m-1)}$. The k^{th} entry of the sequence $\text{ATT}(h_{1:m-1})$ is defined by

$$\text{ATT}(h_{1:m-1})_k := h_k + \frac{1}{Z_k} \sum_{l=1}^{m-1} \exp(\langle Qh_k, Kh_l \rangle_{\mathbb{R}^c}) Vh_l, \quad (5.2a)$$

$$Z_k := \sum_{j=1}^{m-1} \exp(\langle Qh_k, Kh_j \rangle_{\mathbb{R}^c}), \quad (5.2b)$$

where $Q, K \in \mathbb{R}^{c \times d_e}$ and $V \in \mathbb{R}^{d_e \times d_e}$. Note that the output sequence at *any* location k depends on the input sequence at *every* location $l = 1, \dots, m-1$.

We introduce the map $\mathbf{N} : \mathbb{R}^{d_e} \rightarrow \mathbb{R}^{d_e}$, representing a normalization procedure, and extend it to map $\mathbf{N} : \mathbf{F}_e^{(m-1)} \rightarrow \mathbf{F}_e^{(m-1)}$ by allowing it to act pointwise on elements in the input sequence. Similarly, we introduce map $\mathbf{NN} : \mathbb{R}^{d_e} \rightarrow \mathbb{R}^{d_e}$, representing a neural network, and extend it to map $\mathbf{N} : \mathbf{F}_e^{(m-1)} \rightarrow \mathbf{F}_e^{(m-1)}$, again by allowing it to act pointwise on elements in the input sequence. Examples 5.2 and 5.3 describe normalizations and neural networks that are used in practice.

The *attention block* $\mathbf{A} : \mathbf{F}_e^{(m-1)} \rightarrow \mathbf{F}_e^{(m-1)}$ is then defined by the following concatenation of

operations:

$$h_{1:m-1} \leftarrow \text{ATT}(h_{1:m-1}) \quad (5.3a)$$

$$h_{1:m-1} \leftarrow \mathbf{N}(h_{1:m-1}), \quad (5.3b)$$

$$h_{1:m-1} \leftarrow h_{1:m-1} + \mathbf{NN}(h_{1:m-1}), \quad (5.3c)$$

$$h_{1:m-1} \leftarrow \mathbf{N}(h_{1:m-1}). \quad (5.3d)$$

Remark 5.1. The matrices Q, K and V are often referred to in the applied literature as query, key and value matrices [97]. Note that the same matrices define the attention map, and hence the attention block, independently of m . The maps defining the normalization and neural networks are defined pointwise for each element of the sequences to which they are applied, and hence the parameters defining these maps are also independent of m . The independence of these parameters with respect to m is central to having a single parameter ϑ in the definition of the architecture, and in particular in \mathbf{q}_m as defined in (3.4). The complete specification of ϑ is given in Remark 5.7.

Example 5.2 (Layer Normalization). Define a diagonal matrix $D \in \mathbb{R}^{d_e \times d_e}$ and vector $b \in \mathbb{R}^{d_e}$, which are learnable parameters. Layer normalization $\mathbf{N}: \mathbb{R}^{d_e} \rightarrow \mathbb{R}^{d_e}$ applies the rescaling:

$$\mathbf{N}(u) = D \frac{(u - m(u))}{\sqrt{\sigma^2(u) + \varepsilon}} + b, \quad (5.4)$$

where $m(u) = \sum_{i=1}^{d_e} u_i$ and $\sigma^2(u) = \sum_{i=1}^{d_e} (u_i - m(u))^2$, and $\varepsilon > 0$ is a small parameter included for numerical stability. We define $\theta_{\mathbf{no}} = (D, b)$, the learnable parameters of the normalization map \mathbf{N} . Usually ε is user prescribed, not learned.

One simplification does not involve mean shift, diagonal rescaling, shift and stabilization; if we make the choices $\varepsilon = 0$, $b = 0$, $m(u) = 0$ and $D = I$, then we obtain the map given by

$$\mathbf{N}(u) = \frac{u}{\|u\|_2}. \quad (5.5)$$

This is known as root mean square normalization (RMSNorm). This operation constrains the output to the unit sphere: $\mathbf{N}: \mathbb{R}^{d_e} \rightarrow \mathbb{S}^{d_e-1}$. In this case, there are no learnable parameters in the map \mathbf{N} .

Example 5.3 (Neural Network). Often, \mathbf{NN} is implemented as a two layer feed-forward neural network of the form

$$\mathbf{NN}(x) = W_2 \text{act}(W_1 x + b_1) + b_2,$$

where $W_1 \in \mathbb{R}^{c' \times d_e}$, $W_2 \in \mathbb{R}^{d_e \times c'}$, $b_1 \in \mathbb{R}^{c'}$ and $b_2 \in \mathbb{R}^{d_e}$ and where $\text{act}: \mathbb{R} \rightarrow \mathbb{R}$ is an activation function [43], such as ReLU, extended to act pointwise on $\mathbb{R}^{c'}$; integer c' is a user-prescribed channel width, typically different from channel width c in the definitions of matrices Q, K . Then, $\theta_{\mathbf{nn}} = (W_1, W_2, b_1, b_2)$ defines the learnable parameters entering \mathbf{NN} .

5.2. Set Transformer

In this subsection we explain how the attention block from Subsection 5.1 can be used to define the next-token probability model $\mathbf{q}_m(\cdot | \cdot; \vartheta) : \mathcal{F}_e^{(m-1)} \rightarrow \mathcal{P}(\mathcal{V})$. The key component is the *set transformer* $\mathbf{T} : \mathcal{F}_e^{(m-1)} \rightarrow \mathbb{R}^{d_e}$ defined by

$$\mathbf{T}(h_{1:m-1}) = \mathbf{P} \circ \mathbf{A}_K \circ \dots \mathbf{A}_1(h_{1:m-1}); \quad (5.6)$$

here $A_k: F_e^{(m-1)} \rightarrow F_e^{(m-1)}$ are attention blocks, as described in Subsection 5.1, with different parameters for each $k \in S^K$, and the *pooling* operator $P: F_e^{(m-1)} \rightarrow \mathbb{R}^{d_e}$ is now defined.

The pooling operator $P: F_e^{(m-1)} \rightarrow \mathbb{R}^{d_e}$ is a function acting on a sequence and returning a vector. In the context of the set transformer, P is typically chosen to be both permutation-invariant and to be defined for input sequences of arbitrary length. The following example contains two widely used choices that satisfy these properties.

Example 5.4. *The mean pooling operation is given by taking the average of the sequence elements:*

$$P(h_{1:m-1}) = \frac{1}{m} \sum_{k=1}^m h_k.$$

The max pooling operation is given by choosing the maximum along each coordinate of the sequence:

$$P(h_{1:m-1})_j = \max((h_1)_j, \dots, (h_m)_j), \quad j = 1, \dots, d_e.$$

We now introduce the softmax function, using it here to convert elements of \mathbb{R}^V into points on the probability simplex $\mathcal{P}(V)$. Here $\mathcal{P}(S^d)$ denotes the set of probability measures on sets of cardinality d , labeled without loss of generality by the integers S^d .

Definition 5.5. *For any integer d , let $\sigma: \mathbb{R}^d \rightarrow \mathcal{P}(S^d)$ be the softmax function defined as*

$$\sigma(z)_k = \frac{e^{z_k}}{\sum_{j=1}^d e^{z_j}}.$$

Given the set transformer $T: F_e^{(m-1)} \rightarrow \mathbb{R}^{d_e}$, together with linear operator $B: \mathbb{R}^{d_e} \rightarrow \mathbb{R}^{|V|}$, we define $q_m(\cdot | h_{1:m-1}; \vartheta) \in \mathcal{P}(V)$ by

$$q_m(\cdot | h_{1:m-1}; \vartheta) = \sigma(B \circ T(h_{1:m-1}) / \tau). \quad (5.7)$$

Here, $\tau > 0$ is a *temperature* parameter. Choosing τ small leads to greater concentration of the output probability distribution on the most probable tokens under the learned model, whilst larger τ leads to greater variability in the output; this is discussed in Remark 6.2.

Remark 5.6. *Note that it is possible to dispense with B if T were designed to map to $\mathbb{R}^{|V|}$ rather than to \mathbb{R}^{d_e} . However the object $T: F_e^{(m-1)} \rightarrow \mathbb{R}^{d_e}$ as defined is useful for other tasks, different from next-token prediction, which is why we have defined B and T separately. The process of using T in related tasks is known as transfer learning; see [75] for an application of pre-trained text transformers to downstream tasks such as semantic analysis and summarization.*

Remark 5.7. *Taken together, the parameters appearing in all the attention blocks $\{A_k\}_{k=1}^K$, together with the parameters defining linear map B , define the learned parameters ϑ appearing in the next-token prediction model. The parameter $\tau > 0$ is typically not learned, but is user-specified; see Remark 6.2.*

5.3. Encoding Temporal Structure

There are several features of the attention map, all related to temporal structure, which are noteworthy and which suggest modifications of the basic attention map as defined in the previous subsection. These relate to a permutation property of the attention map, to the lack of causality in the attention map, and to the undesirable quadratic scaling of the attention map with respect to sequence length.

5.3.1. Positional Encoding

The map ATT defined in (5.2) is permutation equivariant with respect to elements of the input sequence: applying a permutation to the sequence before applying ATT , and then applying the inverse of the permutation afterward, yields the same result as simply applying ATT . Consequently, such a map discards any positional information in the sequence. The goal of *positional encoding* is to incorporate information on the location of each element in the sequence. Arguably the simplest way to do this is to take $h \in \{f : \mathbb{S}^M \rightarrow \mathbb{R}^{d_e}\}$ and map it to $h' \in \{f : \mathbb{S}^M \rightarrow \mathbb{R}^{d_e+1}\}$ by defining $h'_m = (m, h_m^\top)^\top$. Generalization of this idea to functions varying over open subsets of \mathbb{R}^d is widely used in applications of artificial intelligence to problems arising in science. However, in LLMs different ideas are used and we now outline how they are defined.

The prevailing methodology in LMMs is to map $h \in \{f : \mathbb{S}^M \rightarrow \mathbb{R}^{d_e}\}$ to $h' \in \{f : \mathbb{S}^M \rightarrow \mathbb{R}^{d_e}\}$ by setting $h'_m = h_m + r_m$ where $r : \mathbb{S}^M \rightarrow \mathbb{R}^{d_e}$ computes the *absolute positional encoding* as a function of the index in the sequence. The embedding can be learned using independent parameters for each input index, or contain a small number learnable parameters.

Example 5.8 (Trigonometric Functions). *Given an even dimension d_e , the trigonometric embedding is defined as follows. Set $\lambda_j := 2^{2j/d_e}$ for $j = 1, \dots, d_e/2$ and then*

$$r_m = (\sin(m/\lambda_1), \cos(m/\lambda_1), \sin(m/\lambda_2), \cos(m/\lambda_2), \dots, \sin(m/\lambda_{d_e/2}), \cos(m/\lambda_{d_e/2})).$$

5.3.2. Modified Inner-Product To Address Positional Encoding

When evaluating the attention map (5.2), on sequence $h \in \mathbb{F}^{m-1}$, it is necessary to compute

$$\langle Qh_k, Kh_l \rangle_{\mathbb{R}^c}. \quad (5.8)$$

The inner-product (5.8) can also be adjusted to reflect temporal structure, and in particular to address the issue of positional encoding. Recall the additive function $r : \mathbb{S}^M \rightarrow \mathbb{R}^{d_e}$ defined in the previous subsubsection, and here set this additive function to zero: $r \equiv 0$. Instead, *relative embedding* defines a weighted inner-product based on the distance between the Euclidean image of tokens in the sequence; in this sense it is a positional encoding. The RoFormer in [88] sets absolute positional encoding sequence $r \equiv 0$ and replaces the Euclidean inner-product (5.8) appearing in (5.2) by

$$\langle Qh_k, Kh_l \rangle_{\mathbb{R}^c, \text{roformer}} := \text{Re} \left[\sum_{j=1}^c (Qh_k)_j^\top (Kh_l)_j e^{i(k-l)\psi_j} \right];$$

here $\text{Re}(\cdot)$ denotes taking the real part of the argument. The complex weight accounts for the relative position of the inputs: the ψ_j are chosen to decay as $\gamma^{-2j/d}$ for a large constant γ , resulting in more oscillatory modes for elements that are more separated in the sequence.

5.3.3. Modified Inner-Product To Reduce $\mathcal{O}(m^2)$ Complexity

Modification of the inner-product, introduced in the preceding subsubsection, can be used for a different purpose: to address the issue of reducing complexity, in m , of evaluating the attention map (5.2). When evaluating this map on a sequence $h \in \mathbb{F}^{m-1}$ it is necessary to compute the inner-product (5.8) for all $1 \leq k, l \ll m-1$. Thus, $(m-1)^2$ inner-products must be calculated. *Causal attention* defines the attention map in (5.2) by replacing the inner-product in (5.8) with

$$\mathbb{1}_{l \leq k} \langle Qh_k, Kh_l \rangle_{\mathbb{R}^c}.$$

The masking implied by the indicator function ensures that it is only necessary to compute $(m-1)(m-2)/2$, rather than $(m-1)^2$, inner-products. More generally, given an adjacency matrix $A \in \{0, 1\}^{(m-1) \times (m-1)}$, *sparse attention* maps replace (5.8) with

$$A_{lk} \langle Qh_k, Kh_l \rangle_{\mathbb{R}^c}.$$

The adjacency matrix ensures that interactions between sequence elements are only computed when $A_{kl} \neq 0$. For example, given a bandwidth $r > 0$, we can consider a banded adjacency matrix that has nonzero entries only for A_{kl} with $|k - l| \leq r$. For a bandwidth $r \ll m - 1$, the complexity of computing the attention map will then scale linearly with the sequence length as $\mathcal{O}(r(m-1))$; see Section 1.2 for references to recent computational methodologies with linear dependence.

5.3.4. Replacing The Attention Map To Reduce $\mathcal{O}(m^2)$ Complexity

The previous subsubsection shows how both causality, and the related wish to obtain linear scaling in m , can be achieved (separately) by selecting a subset of the $(m-1)^2$ inner-products required to define the attention map (5.2), and setting all others to zero. An approach to achieving both of these goals simultaneously is through *state-space models*. These work by replacing $\text{ATT} : \mathbb{F}_e^{(m-1)} \rightarrow \mathbb{F}_e^{(m-1)}$ in the attention block with a different sequence-to-sequence map $\text{SSM} : \mathbb{F}_e^{(m-1)} \rightarrow \mathbb{F}_e^{(m-1)}$. This map is defined by the following iteration, for $k = 0, \dots, m-2$:

$$v_{k+1} = f(v_k, h_k; \theta^f), \quad v_0 = v, \quad (5.9a)$$

$$\text{SSM}(h_{1:m-1})_{k+1} = g(v_{k+1}, h_{k+1}; \theta^g). \quad (5.9b)$$

Here each $v_k \in \mathbb{R}^{c''}$ for some preselected channel width c'' . Notice that $v_{0:m-1}$ accumulates information about the sequence $h_{1:m-1}$, but does so in a causal fashion: v_{k+1} depends only on $h_{1:k}$. Thus $\text{SSM}(h_{1:m-1})_{k+1}$ depends only on $h_{1:k+1}$. The parameters v , θ^f and θ^g are learned. The complexity of evaluating $\text{SSM}(h_{1:m-1})$ is linear in m . In practice, the model is often implemented using linear f, g , defined through discretizing a linear and continuous time analog of (5.9); details may be found in Appendix C. State space models have produced state-of-the-art performance on audio and genomics datasets for sequences of length $\mathcal{O}(10^6)$. However, they are currently not competitive with attention based architectures for typical language tasks.

6. Sequence Generation

In Section 3 we described the framework for next-token prediction. Here we detail how it may be used to generate text sequences. Recall that LLMs roll out sequences in V step-by-step, starting with a sequence of a given length, then generating a sequence of length one greater, and increasing the sequence length by one in steps until it reaches length L . The basic building block for this roll-out is the learned model (6.1) which we recall here. Combining (3.3) and (3.4), and deploying the optimal choice $\theta^* = (\vartheta^*, \varphi^*)$ found through (typically only approximately) minimizing $\mathcal{L}^N(\theta)$ as defined in (4.5), we obtain

$$\pi_{1:L}(f_{1:L}; \theta^*) = \prod_{\ell=1}^L \pi_m(f_\ell | f_{1:\ell-1}; \theta^*), \quad (6.1a)$$

$$\pi_m(f_\ell | f_{1:\ell-1}; \theta^*) = q_m(f_\ell | \phi^* \circ f_{1:\ell-1}; \vartheta^*); \quad (6.1b)$$

here ϕ^* is given by function ϕ from Definition 2.6, with $\phi = \phi^*$ defined by choice $\varphi = \varphi^*$. The process of deploying (6.1) to generate a sequence of increasing length starting from an input sequence is

known as *decoding*. Subsection 6.1 describes how this decoding is started and how it is stopped. In Subsection 6.2 we consider deterministic techniques for sequence generation between the starting and stopping points, based on maximizing probabilities in (6.1). Subsection 6.3 is devoted to randomized techniques for doing so, based on sampling. And in Subsection 6.4 we illustrate how these two approaches may be combined.

6.1. Starting and Stopping The Decoding

In general, the model in (6.1) will be deployed by rolling out next-token prediction, starting from a given text *prompt*. Examples of applications of LLMs, and the choice of prompts for these applications, are presented in Section 7. Here we simply assume that the prompt is given and comprises a sequence $f_{1:\ell_{\text{prompt}}}^{\text{prompt}}$ for some $\ell_{\text{prompt}} < L$. We define $\mathcal{F}^{L,\text{prompt}} \subset \mathcal{F}^L$ by

$$\mathcal{F}^{L,\text{prompt}} = \{f \in \mathcal{F}^L : f_m = f_m^{\text{prompt}}, m = 1, \dots, \ell_{\text{prompt}}\} \quad (6.2)$$

The prompting sequence $f_{1:\ell_{\text{prompt}}}^{\text{prompt}}$ is, in some settings, referred to as the *context*. To separate the prompt from the generated text, a special token in the vocabulary known as **beginning of sequence** (BOS) is often used in element ℓ_{prompt} of the sequence.

We may then use next-token prediction based on (6.1) to find sequences conditioned on being in $\mathcal{F}^{L,\text{prompt}}$. One of the tokens in the vocabulary is the **end of sequence** (EOS) token which typically arises at some step L_{stop} satisfying $\ell_{\text{prompt}} < L_{\text{stop}} \leq L$. When this token arises, the LLM's response to the prompt is essentially complete. However a special **padding** (PAD) token is used in each of the remaining entries of the sequence, in order to build a sequence of the standardized length L .⁴ This padding corresponds to defining a transition probability in (6.1b) which is a Dirac measure on the padding token whenever the conditioning sequence contains an EOS token.

From a probabilistic point of view, the preceding procedure corresponds to *conditioning* the next-token prediction model (6.1) on the sequence $f_{1:\ell_{\text{prompt}}}^{\text{prompt}}$. This sequence on which we condition generates the σ -algebra $\mathcal{F}^{L,\text{prompt}}$.

6.2. Deterministic Generation

The model (6.1) for next-token prediction is probabilistic. However, it may be desirable to derive from it a deterministic method for sequence generation, given a prompt. One natural deterministic approach to using it is to seek the most likely sequence under the learned model, given the text prompt:

$$(f_1, \dots, f_L) \in \arg \max_{f \in \mathcal{F}^{L,\text{prompt}}} \pi_{1:L}(f; \theta^*). \quad (6.3)$$

For a discrete state-space where each token can take one of $|\mathcal{V}|$ elements in the vocabulary, identifying the optimal sequence solving (6.3) can, in principle, be found by enumeration: computing the probability for all $|\mathcal{V}|^{L-\ell_{\text{prompt}}}$ possible sequences and picking the one with maximum probability under the joint model. However, the computational cost of this procedure grows exponentially with L and as a result it is intractable to solve (6.3) in practice.

An alternative, tractable, approach is to use the auto-regressive factorization of the joint probability distribution in (6.1). We solve the sequence of optimization problems

$$f_m \in \arg \max_{v \in \mathcal{V}} \pi_m(v | f_{1:m-1}; \theta), \quad m = \ell_{\text{prompt}} + 1, \dots, L; \quad (6.4)$$

⁴Often this standardized length is in fact defined as $L + \ell_{\text{prompt}}$, rather than L , as the prompt is not viewed as part of the response.

this rolls-out the desired sequence. Performing each optimization step requires computing the $|\mathcal{V}|$ probabilities for the elements in the vocabulary, leading to cost that scales as $|\mathcal{V}| \times (L - \ell_{\text{prompt}})$. This procedure is known as *greedy decoding*. In general, the greedy procedure is sub-optimal with respect to the globally optimal solution in (6.3). In particular, there may exist high probability paths that are hidden by greedily picking the most likely next-token and not considering a lower probability choice that results in a better overall solution when considering an entire sequence. We emphasize that the greedy solution does not change past elements of the sequence after they have been generated.

Example 6.1. *To ameliorate this effect, beam search optimizes on a windowed sequence of fixed, short length ℓ greater than one [34]. To describe the method precisely we define $\pi_{m:m+\ell-1}(\cdot | f_{1:m-1})$ to be the probability distribution on sequence $f_{m:m+\ell-1} := (f_m, \dots, f_{m+\ell-1})$ of length ℓ implied by the autoregressive model (3.1). The method approximates the probability distribution on this sequence, and maximizes over it. For example the basic version of beam search with $\ell = 2$ chooses elements at step m by solving the two-dimensional optimization problem:*

$$f_{m:m+1} \in \arg \max_{(v, v') \in \mathcal{V} \times \mathcal{V}} \pi_{m:m+1}(v, v' | f_{1:m-1}), \quad m = \ell_{\text{prompt}} + 1, \dots, L - 1.$$

This has cost that scales as $|\mathcal{V}|^2$. In practice the search is restricted to avoid the quadratic complexity in the number of tokens. This is typically done by restricting the search related to f_m to a subset of elements from \mathcal{V} with total size $k \ll |\mathcal{V}|$, which is determined based on greedy search. This restriction reduces the complexity of the two-dimensional optimization problem to $k|\mathcal{V}|$ leading to an overall cost that scales as $k|\mathcal{V}| \times (L - \ell_{\text{prompt}})$ for generation of the entire sequence. Although more expensive than the basic greedy approach, the improved quality of the decoded sequence, for example in code generation [34], may justify the approach in some settings.

6.3. Stochastic Generation

Rather than adopting a deterministic approach to sequence generation by identifying some point of maximum probability, an alternative is to sample from $\pi_{1:L}(f_{1:L}; \theta^*)$, conditioned on the sequence being in $\mathcal{F}^{L, \text{prompt}}$. It is possible to draw exactly from this conditional probability distribution by using next-token prediction as follows:

$$f_m \sim \pi_m(\cdot | f_{1:m-1}; \theta), \quad m = \ell_{\text{prompt}} + 1, \dots, L.$$

Throughout this procedure $f_{1:\ell_{\text{prompt}}}$ is fixed at the prompt $f_{1:\ell_{\text{prompt}}}^{\text{prompt}}$, ensuring that the generated sequence is in $\mathcal{F}^{L, \text{prompt}}$.

Remark 6.2. *Recall that a user-specified temperature parameter τ is chosen to define the learned next-token probability model: see (5.7). It is not uncommon for this parameter to be chosen differently when decoding than when training the model. Choosing temperature $\tau \ll 1$ when decoding increases the weight associated to the most likely token; hence the distribution over tokens becomes more concentrated. In the limit of $\tau \rightarrow 0$, the sampling procedure reduces to the greedy deterministic procedure described in the previous subsection. Choosing larger τ increases the probability of sampling rare tokens and hence the diversity of outputs from the LLM.*

6.4. Mixing Deterministic and Stochastic Generation

There are numerous ways of mixing the deterministic and stochastic approaches to decoding. A simple example is to consider sampling the first L' tokens, in positions $\{\ell_{\text{prompt}} + 1, \dots, \ell_{\text{prompt}} + L'\}$,

and thereafter use greedy decoding:

$$f_m \sim \pi_m(\cdot | f_{1:m-1}; \theta), \quad m = \ell_{\text{prompt}} + 1, \dots, \ell_{\text{prompt}} + L'$$

$$f_m \in \arg \max_{v \in V} \pi_m(v | f_{1:m-1}; \theta), \quad m = \ell_{\text{prompt}} + L' + 1, \dots, L.$$

Remark 6.3. In Subsection 7.1 we introduce chain-of-thought reasoning as a methodology to improve the quality of responses provided by an LLM. In [103] mixed deterministic and stochastic generation, with $L' = 1$, is used in this context. Introducing stochasticity in the first token is found to increase diversity, and resulting accuracy, of the responses.

7. Applications Of Autoregressive LLMs

In this section, we demonstrate how LLMs may be employed for various tasks. In order to present a consistent picture, our illustrations use the Qwen-2.5 model with 3B parameters [52], accessed in November 2025. Unless we state otherwise, this algorithm is deployed using the greedy decoding procedure, for sequence generation, that we described in Section 6.2. We illustrate question answering and conversation (Subsections 7.1 and 7.2), mathematical problem solving (Subsection 7.3), the generation of computer code (Subsection 7.4), translation between different languages (Subsection 7.5), text summarization (Subsection 7.6) and multimodal data processing (Subsection 7.7).

In showcasing these applications of LLMs we will not only highlight the variety of tasks for which LLMs may be used, but we will also focus on shortcomings of the methodology; furthermore, we will describe approaches to address these shortcomings. Underlying these shortcomings is the inability to impose logical constraints within an LLM; we will describe approaches such as chain-of-thought reasoning, in-context learning and fine-tuning which are used to address this lack of logical constraint. All these approaches may be seen as attempts to increase the probability of achieving desirable, or logically consistent, responses from the LLM, with respect to randomness inherent in the sequence generation, or with respect to a probability measure on the prompts used to generate a response. In studying multi-modal processing we will also introduce encoder-decoder pairs, enabling LLMs to exploit other data modalities such as images, audio and video⁵.

7.1. Question Answering

In this section we present examples of prompting the LLM with questions that, for a human, require logical reasoning to provide an answer. It is therefore of interest to study the performance of the LLM since the LLM is based entirely on a probabilistic model of next-token prediction, and has no logical constraints on its output. We start with the following example:

```
"prompt": A man named Frank travels from NYC to Philadelphia by road, on a
Monday, leaving at 9:00am and arriving at 12noon. He then travels from
Philadelphia to NYC the next day, Tuesday, also leaving at 9:00am and arriving
at 12 noon. He takes the same route, but on Tuesday reverses the route taken
on Monday. Is it necessarily the case that there is at least one point that he
will be located at the same time, albeit on the two different days? Just give
a Yes or No answer.
"output": Yes<|endoftext|>
```

This answer is correct and so it might appear to a casual user that the LLM is able to apply logical reasoning; but as we know this is not, in fact, the case. We probe this issue by introducing

⁵Code to reproduce all of the examples can be found at: <https://github.com/baptistar/LLMExamples>.

the concept of Chain-of-Thought (CoT) reasoning. This refers to a group of techniques that are used to improve the ability of LLMs to solve complex problems by including reasoning within their response. The simplest strategy to achieve this is by appending to the prompt an instruction such as “Explain your answer”. We now study the output of the model, in response to the same question about Frank’s journeys, but now where the model is additionally prompted to include a step-by-step explanations. Perhaps the most succinct explanation for the correct answer of “yes” is to explain that the question is logically equivalent to one in which two distinct people make the journey at the same time on the same day; once this logical equivalence is noted it is clear that they must therefore cross paths at least once. However, as the response in Appendix E.1 shows, the LLM provides a rather verbose answer, centered around the intermediate-value theorem, when asked to provide its reasoning. Furthermore the response contains dubious statements such as “Since he [Frank] takes the same route on both days, his position as a function of time will be continuous.”

Remark 7.1. *Despite the mixed response shown in Appendix E.1, there are settings in which CoT reasoning has measurable positive effect on the correctness of the final answer. The potential benefits from using the approach are highlighted in [103].*

CoT reasoning attempts to impose logical structure, approximately, by guiding the LLM to provide *output* which explains the answer to the question. In contrast, In-context Learning (ICL), described in Subsection 7.3, supplements the *input* to the LLM in a manner which aims to impose logical structure, approximately. The word *approximately*, in both cases, can be interpreted as increasing the probability that the LLM produces the correct answer to the question at hand; or to an increase in the probability that the LLM produces a logically consistent reasoning leading to the correct answer. This probabilistic notion of accuracy is to be interpreted with respect to the inherent probabilistic nature of next-token prediction and with respect to a probability distribution on prompts; see Section 8.

7.2. Conversations

The previous section demonstrates question and answering where there is a definitive, logically correct, answer. In this subsection, we describe question and answering in a different context: prompts which require extraction of knowledge contained in the data used to train the LLM. We also use this setting to illustrate conversing with an LLM, when a user requests refinement of the original question. We arrange the discussion around Bayes’ theorem:

```

"prompt": Explain Bayes' theorem simply without formulas.
"output": Bayes' theorem is a way to update our beliefs about something based on
new information. It helps us figure out how likely an event is, given some
evidence.<|endoftext|>

```

The answer is reasonable and can be followed up to ask for more technical detail; the output for a follow-up question that requests a formal presentation of Bayes’ theorem is provided in Appendix E.2. The response given there is factually correct, succinct and describes some context as well as the underlying mathematics. It is notable that complex knowledge of this type is encoded in the capabilities of an LLM and can be extracted by next-token prediction.

Taken together, the example in this subsection and the linked appendix demonstrate the impressive abilities of LLMs to extract knowledge, using next-token prediction. On the other hand, the examples in Subsection 7.1 and follow-up in the appendix demonstrate the potential pitfalls related to the lack of logical constraints on the next-token prediction methodology.

Remark 7.2. *The text explaining Bayes’ theorem is generated from an LLM that was trained on a static data-set from a particular point of time in the past. Since Bayes’ theorem itself does not change with time, this does not present a problem. However, for some queries, such as planning an itinerary for a vacation, or preparation of a legal document, it can be important to access up-to-date information from the internet. In this context, a particularly effective use of fine-tuning (a concept introduced in Subsection 4.3) is a methodology known as retrieval-augmented generation [62]. Fine-tuning can, for example, be used to incorporate knowledge from Wikipedia. The version of Qwen that we consistently deploy in this paper does not have this capability; but other more recent versions do.*

7.3. Mathematics

The reader who has followed our development of LLMs based on next-token prediction will be aware that there is no constraint of logical consistency imposed by the methodology. For example there is nothing to prevent an LLM implying, or even explicitly stating, as part of a response, that $2*2=5$. The probability of it doing so might well be low; but there is no hard constraint to prevent it. In this subsection we probe the ability of LLMs to tackle tasks in mathematics. The lack of logical constraints presents as a significant barrier in this arena.

An important general concept when using LLMs is the question of how to incorporate additional prior knowledge, relevant to a specific limited set of tasks, to improve the performance of the LLM. One approach is through fine-tuning, the methodology outlined in Subsection 4.3, and as studied through an example in Subsection 7.4. A second approach is through ICL, discussed above, and which we now illustrate in detail in the context of mathematical problem solving.

ICL works by adding, to the input, text known as *context* which aims to guide the LLM so that next-token prediction gives desirable output. To illustrate this idea, we consider specific multiplication problems such as 473×45 . Without context the LLM provides the incorrect answer 21385. With appropriately chosen context, it provides the correct answer 21285. In Appendix E.3 we show how the basic LLM arrives at its incorrect answer, we show the context from [22] that we used, and we show how the LLM, equipped with this context, arrives at the correct answer. In the same appendix, we also show the model output with stochasticity and how the inclusion of stochasticity leads to an improved probability of producing the correct answer, with and without ICL.

Remark 7.3. *CoT thought reasoning can be combined with ICL, providing not only examples of response to similar prompts, but also ensuring that the examples themselves have step-by-step responses. The use of specialized sampling strategies that elicit a reasoning path, rather than generation of deterministic sequences, typically leads to answers that contain fewer factual errors or logical inconsistencies. As with our discussion at the end of Subsection 7.1, such statements about improved approximation of the desired response, should be interpreted probabilistically.*

7.4. Coding

We now illustrate the use of LLMs to generate computer code. We highlight the role of fine-tuning, introduced in Subsection 4.3, a methodology for introducing task-specific information to improve an LLM. In contrast to ICL, which employs additional information at the time that the LLM is deployed, fine-tuning uses additional information in a second training phase; see [52] for the details of the coding-specific dataset consisting of over 5.5 trillion tokens that was used to fine tune the Qwen-2.5-Coder model series. We used the 3B model to generate the following examples.

We give two examples of the LLM response in Appendix E.4, first without fine-tuning, and then with fine-tuning. Both examples produce an ordinary differential equation (ODE) that is integrated

using RK45. This choice coincides with the method that MATLAB recommends as the first choice to solve non-stiff ODEs [94]. However, neither code is general purpose, enabling solution of an arbitrary ODE in \mathbb{R}^n ; instead, a specific example in two dimensions is given. In Appendix E.4 we also include the graphical output produced by both codes when running the MATLAB code to solve the specific second order ODE chosen by next token prediction. We note that while both models produce a valid MATLAB script without syntax errors, the first model, which is not fine-tuned for coding, produces an example whose solution is unstable and blows up in the selected time range.

7.5. Translation

Translation has been a guiding application in the development of LLMs since the field emerged over the last decade. It can be performed by simply using a prompt that requests the translation of a provided piece of text into a specified, different, language. One approach to enhance a general purpose LLM for translation is to use fine-tuning, introduced in Subsection 4.3. Fine-tuning can be performed by using pairs of translated sequences $\{(f_{1:L}^{(n)}, f'_{1:L'}^{(n)})\}_{n=1}^{N_{\text{fine}}}$, where $f_{1:L} \sim p(f_{1:L})$ is a sequence in a given language, and $f'_{1:L'} = \mathcal{T}(f_{1:L})$ where \mathcal{T} is a mapping of the sequence to a different language. We note that a given piece of text will typically be represented by different numbers of tokens in different languages; hence $L' \neq L$ in general. However, current LLMs are so powerful that they can successfully translate, without being fine-tuned for translation; this approach is known as *zero-shot* translation. The example below shows zero-shot translation of a short phrase from English into French, and back again. This example was performed using Qwen2.5-3B-Instruct model, which was fine tuned for improved instruction following, but not for language specifically. It is notable, but should not be surprising, that the map from English to French is not inverted exactly, but only approximately.

```
"prompt": Translate "Thank you for your help with answering my math question."
           into French.
"output": "Merci pour votre aide à répondre à ma question de
          mathématiques."<|im_end|>
"prompt": Translate "Merci pour votre aide à répondre à ma question de
          mathématiques" into English
"output": "Thank you for your help in answering my math question."<|im_end|>
```

7.6. Summarization

LLMs are also used to summarize large corpora of documents that would be time-consuming for humans to process manually. LLMs achieve this task by identifying latent semantic representations of the corpora's content, in some cases using a hierarchical procedure to summarize intermediate summaries to mitigate the context window constraint for large corpora [45, 111]. The following example shows LLMs applied to summarize the introduction (Section 1) of this paper. We omit the introduction in the prompt below for conciseness. We note that it was provided in a LaTeX format, emphasizing the model's ability to process text in various languages and formats.

```
"prompt": Summarize the following introduction section of a paper into a single
          sentence.
"output": This paper aims to present a precise mathematical formulation of large
          language models, elucidating their core methodology and underlying principles
          for a mathematically inclined audience, thereby addressing their current
          shortcomings and offering a foundation for further computational and
          theoretical studies by mathematicians.<|im_end|>
```

7.7. Multimodal Processing And Generation

Multimodal Large Language Models (MLLMs) extend the capabilities of LLMs, which were originally developed for processing text sequences, to other data modalities; typical examples of other data modalities include images, audio and video. MLLMs commonly leverage a pre-trained LLM, often referred to as the *backbone* model, that auto-regressively process and generate elements in \mathcal{F}_e^M , sequences of length M taking values in \mathbb{R}^e , as presented in Sections 2 and 3. In this subsection, we will illustrate MLLMs by describing how to leverage a backbone model for *image understanding*: the task of processing an input image and generating an output text sequence. This procedure will immediately generalize to processing other multimodal data, as well as combinations of data from different modalities. We will then describe one popular multimodal processing task known as *Visual Question Answering* (VQA), where the input contains an image, together with a text prompt containing a question based on the image; and the output is the answer to that question.

7.7.1. Image Understanding

For image understanding, we assume that the image is represented as a sequence $f_{1:M'}^{\text{im}}$ in $\mathcal{F}_{\ell'}^{M'}$: the space of sequences of length M' taking values in $\mathbb{R}^{d_{\ell'}}$. For an example of how different data modalities are represented as a sequence, see Section 2.4; there we have a brief discussion of how an image is represented as a flattened sequence. To process the image, an MLLM first encodes the input sequence in $\mathcal{F}_{\ell'}^{M'}$ into the sequence space for the backbone LLM. This is achieved by defining the map $M^{\text{im}}: \mathcal{F}_{\ell'}^{M'} \rightarrow \mathcal{F}_e^M$. The map is commonly composed of two pieces: $M^{\text{im}} = P^{\text{im}} \circ E^{\text{im}}$. Here E^{im} is a pretrained *encoder* $E^{\text{im}}: \mathcal{F}_{\ell'}^{M'} \rightarrow \mathcal{F}_e^M$ for images; typically this pretraining will have been undertaken independently of the training of the backbone LLM and, as a consequence, typically $d_{\ell} \neq d_e$. The encoder uses specialized architectures for images or other data types; for example a vision transformer is typically used for processing images into a sequence. The map $P^{\text{im}}: \mathcal{F}_e^M \rightarrow \mathcal{F}_e^M$ is based on an elementwise *projector* $P^{\text{im}}: \mathbb{R}^{d_e} \rightarrow \mathbb{R}^{d_e}$, extended to operate on sequences of length M according to the definition $(P^{\text{im}}(f^{\text{im}}))_k := P^{\text{im}}(f_k^{\text{im}})$ for $k = 1, \dots, M$. The projector $P^{\text{im}}(\cdot; \vartheta^{\text{im}})$ is commonly taken to be a feedforward neural network with parameters ϑ^{im} that are chosen to align the range of the encoder with the input space to the LLM. These parameters are identified using a fine-tuning procedure built from the following data.

Data Assumption 7.4. *We collect pairs of images and text sequences drawn i.i.d. from a joint distribution $\{f_{1:M'}^{\text{im},(n)}, f_{1:L}^{(n)}\}_{n=1}^{N_{\text{im}}} \sim p(f_{1:M'}, f_{1:L})$.*

Using this data, we learn the parameters ϑ^{im} of the projector $P^{\text{im}}(\cdot; \vartheta^{\text{im}})$; the parameters of the backbone LLM and the encoder are fixed during this fine-tuning process. The empirical objective function minimized, using the same procedures described in Subsection 4.5, is given by:

$$\mathcal{L}^{N_{\text{im}}}(\theta) = - \sum_{n=1}^{N_{\text{im}}} \log \pi_{1:L}(f_{1:L}^{(n)} | P^{\text{im}}(E^{\text{im}}(f_{1:M'}^{\text{im},(n)}; \vartheta^{\text{im}}); \theta^*)), \quad (7.1)$$

where $\theta := \vartheta^{\text{im}}$ and θ^* denotes the LLM parameters found through pretraining.

After training, the backbone LLM may now be used to generate text in response to an image input, using the generative approaches outlined in Section 6, with the image as a prompt. Given an image, not in the training data, we embed it into Euclidean space using the encoder E^{im} and learned projector P^{im} ; the resulting Euclidean sequence may be used as the prompt for the LLM, as in Subsection 6.1. The generated output tokens can then be decoded into text using the vocabulary.

Remark 7.5. We note that modalities other than images can also be formatted as a Euclidean sequence, enabling generalization of the preceding methodology on image understanding to other tasks such as audio or video understanding. Audio is a sequence natively indexed by time; video may be time-indexed with image (and possibly sound) at each time, although other organizations of the space-time data may also be considered.

This basic idea, to generate text from an image or other data modality, may be further refined. For example, it may be used to provide reasoning or follow instructions based on semantic visual and language information. We now illustrate this idea with VQA.

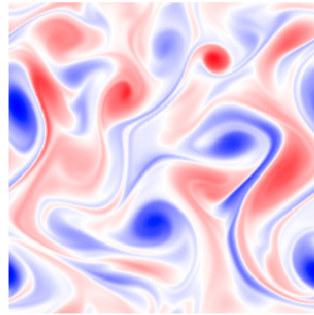
7.7.2. Visual Question and Answering

We now build on the preceding subsubsection to describe VQA: question answering when the question refers to an input image and together the question and image form the prompt. When the input consists of more than one modality, such as a text sequence $f_{1:\ell_{\text{prompt}}}^{\text{prompt}}$ and an associated image $f_{1:\ell_{\text{im}}}^{\text{im}}$, we process each input into the same Euclidean space. After embedding, the text and image are sequences in $\mathcal{F}_e^{\ell_{\text{prompt}}}$ and $\mathcal{F}_e^{\ell_{\text{im}}}$, respectively for $\ell_{\text{prompt}} + \ell_{\text{im}} < L$. By concatenation, we can define the prompting sequence to be:

$$\mathcal{F}^{L,\text{prompt}} = \{f \in \mathcal{F}^L : f_m = f_m^{\text{prompt}}, m = 1, \dots, \ell_{\text{prompt}}, f_m = f_m^{\text{im}}, m = \ell_{\text{prompt}} + 1, \dots, \ell_{\text{prompt}} + \ell_{\text{im}}\}.$$

We can then generate an output text sequence of maximum context length L given the prompt. We now provide an example using the Qwen-3 model for VQA. The following shows an example where the LLM is asked to describe an image from a simulation to the Navier-Stokes equation; see [99] for details on the image. The output text correctly identifies the vortical structures present in the flow and suggests that it might be (decaying) turbulence created by flow past an obstacle or in a channel. These are reasonable suggestions, consistent with the image.

`"prompt": Describe this image representing a solution to Navier Stokes equation.`



`"output": This image is a visualization of a solution to the Navier-Stokes equations, likely representing a two-dimensional turbulent or transitional flow field. While the exact physical context (e.g., flow past an obstacle, channel flow, or decaying turbulence) isn't specified, the visual features strongly suggest it depicts vortical structures and coherent eddies in a fluid.`

Remark 7.6. A MLLM can also be used to generate data from modalities other than text. We illustrate this by explaining how the generated data may itself be an image. (Generalizations to

producing data from other modalities are similar). An example of a problem where this is needed is the use of an LLM to produce an edited image, given a starting image and a description of the features to be changed. Generating image data rather than text data requires a mapping from Euclidean sequences representing text to Euclidean sequences representing images. Recall that in Subsubsection 7.7.1 we have already introduced a map in the converse direction: $M^{im}: F_{\ell'}^{M'} \rightarrow F_e^M$. Here we introduce $D^{im}: F_e^M \rightarrow F_{\ell'}^{M'}$, an approximate inverse. We can use D^{im} to map a (Euclidean representation of a) text sequence to a flattened representation of an image as a Euclidean sequence.

Although we have presented the inverse map as working on Euclidean sequences, for simplicity of exposition, the map D^{im} is typically built from a decoder which works over a discrete vocabulary. This involves creating an (approximate) representation of any image data sample as a sequence over a finite vocabulary, often referred to as a codebook. Note that a finite vocabulary is not used to process image data into text, as described in Subsubsection 7.7.1; it is just needed for generation. Approaches to learn the vocabulary and the decoders include DC-GAN and VQ-VAE for images [72, 77]. The decoder architectures for different data modalities follow a similar structure to the encoder architectures described in Subsubsection 7.7.1 that compose a pre-trained map with fine-tuned projector. Fine-tuning the encoder and decoder parameters requires datasets of paired samples where each sample contains related representations of a common underlying object in every data modality, as in Data Assumption 7.4 for image and text data. This approach has been used to build models that can simultaneously understand and/or generate up to 21 different data modalities [13].

8. Evaluation of LLMs

The preceding sections have shown how LLMs work using probabilistic next token prediction, highlighted their remarkable capabilities across numerous applications of the methodology, and demonstrated shortcomings, in particular in relation to their inability to impose logical structure as hard constraints. Given both the potential wide-ranging uses of LLMs, together with their demonstrable shortcomings, evaluation of them is clearly of importance. This section is devoted to how the question of evaluation may be confronted. In Subsection 8.1 we give an abstract mathematical formulation of evaluation, followed in Subsection 8.2 by citation to papers conducting benchmarking in practice.

8.1. Mathematical Formulation

Recall from (3.1) the true probability distribution defined, in principle, by all available text:

$$p_{1:L}(f_{1:L}) = \prod_{\ell=1}^L p_{\ell}(f_{\ell}|f_{1:\ell-1}). \quad (8.1)$$

From (3.3) and (3.4) we have our approximate probability distribution on text, taking the form:

$$\pi_{1:L}(f_{1:L}; \theta) = \prod_{\ell=1}^L q_{\ell}(f_{\ell}|\phi \circ f_{1:\ell-1}; \theta). \quad (8.2)$$

After application of a specific choice of one of the training procedures detailed in Section 4, a choice θ^* is made for the parameter vector defining the LLM (8.2). This choice is aimed at aligning the LLM with the true probability distribution (8.1). We can now ask for precise measures of the performance of the LLM on specific tasks.

Recall $F^{L,prompt}$ from equation (6.2), representing the σ -algebra on sequences in F^L created by a fixed text prompt $f_{1:\ell_{prompt}}^{prompt}$. This text prompt may contain in-context information; see Section 7.3. Given a specific text prompt defining $F^{L,prompt}$ we might be interested in the difference between

the conditional probabilities $p_{1:L}(f_{1:L}|\mathcal{F}^{L,\text{prompt}})$ and $\pi_{1:L}(f_{1:L}; \theta|\mathcal{F}^{L,\text{prompt}})$. Using a divergence $D : \mathcal{P}(\mathcal{F}^L) \times \mathcal{P}(\mathcal{F}^L) \rightarrow \mathbb{R}^+$, we define a measure of the effectiveness of the LLM, for this specific text prompt, to be

$$E(f_{1:\ell_{\text{prompt}}}^{\text{prompt}}) := D\left(p_{1:L}(f_{1:L}|\mathcal{F}^{L,\text{prompt}}) \parallel \pi_{1:L}(f_{1:L}; \theta^*|\mathcal{F}^{L,\text{prompt}})\right). \quad (8.3)$$

This divergence quantifies the difference between the “true” distribution of responses (constrained to have total length less than L) given a specific prompt, and the distribution of the LLM, given the same prompt. Averaging over text prompts from a given distribution π^{prompt} , noting that such a distribution will typically be over prompts of different lengths, gives a measure of the average effectiveness of a trained LLM over a class of prompts:

$$e = \mathbb{E}_{f_{1:\ell_{\text{prompt}}}^{\text{prompt}} \sim \pi^{\text{prompt}}} E(f_{1:\ell_{\text{prompt}}}^{\text{prompt}}). \quad (8.4)$$

The choice of distribution on text prompts defines a class of problems of interest. The choice of D is crucial in making evaluation of the effectiveness feasible in practice.

Example 8.1. *A natural choice for D in (8.3) is the KL divergence (4.1) between the approximate model distribution and the data distribution; this leads to the same objective used to train the LLM in Section 4, constrained by the specific text prompt. Making this choice and evaluating the average effectiveness e given in (8.4) leads to*

$$e = \text{const} - \mathbb{E}_{f_{1:\ell_{\text{prompt}}}^{\text{prompt}} \sim \pi^{\text{prompt}}} \mathbb{E}_{f_{1:L} \sim p_{1:L}(\cdot|\mathcal{F}^{L,\text{prompt}})} \log \pi_{1:L}(f_{1:L}; \theta^*|\mathcal{F}^{L,\text{prompt}});$$

here const is a scalar that is independent of the model parameters θ^* . Thus, the following second term can be used to compare the effectiveness of two different parameter values:

$$-\mathbb{E}_{f_{1:\ell_{\text{prompt}}}^{\text{prompt}} \sim \pi^{\text{prompt}}} \mathbb{E}_{f_{1:L} \sim p_{1:L}(\cdot|\mathcal{F}^{L,\text{prompt}})} \log \pi_{1:L}(f_{1:L}; \theta^*|\mathcal{F}^{L,\text{prompt}}).$$

In particular, a lower value for the preceding expressions indicates that the approximate model is closer in KL divergence to the data distribution. An empirical estimate of this expression, given i.i.d. samples of prompts and responses drawn from the data distribution, is referred to as the negative log-likelihood or cross-entropy of the model. The exponentiated negative log-likelihood of a single sequence is often referred to as perplexity.

Example 8.2. *Another potentially useful choice of D is the energy distance or maximum mean discrepancy (MMD). This is because both can be evaluated using only samples; see [12, Chapter 11]. Evaluating the effectiveness $E(f_{1:\ell_{\text{prompt}}}^{\text{prompt}})$ using the energy distance or MMD, for a given prompt, requires generating samples from the approximate model and collecting samples from the data distribution which are consistent with the prompt. In practice, the samples may not have the same length so it may be advantageous to project both samples into a common space. For example, we may ask the LLM for a “Yes/No” response and process each sample from the data distribution in a binary space prior to computing the divergence.*

For logical problems with a single, correct response, we can compare the modeled distribution with a specific answer. This can be achieved using scoring-rules $S : \mathcal{P}(\mathcal{F}^L) \times \mathcal{F}^L \rightarrow \mathbb{R}$ which compare a distribution to a point. Examples of scoring rules include continuous ranked probability score (CRPS) or the energy score⁶. The expectation of the scoring rule over a distribution on the point can be used to define a divergence. See [12, Chapter 11] for the definitions and details of these rules.

⁶In one dimension, for example, the CRPS computes the square of the L^2 norm of the difference between the cumulative distribution function (CDF) of the distribution and the CDF of a Dirac mass at the point.

When applying LLMs to problems with a single correct response, this will be the point that enters the scoring rule; the distribution will be that of the LLM.

For evaluation of logical problems with a single correct response, another approach is to summarize the modeled probabilities with a single point. This, for example, might be the answer implied by the output of the greedy decoding algorithm defined by (6.4); and then this point is compared directly with the correct response in some metric or, if the answer is numerical, a norm. When the model is used to retrieve a set of information, its output can also be evaluated by counting the number of true positives, false positives, and false negatives in the output relative to a ground-truth set. These counts are often used to report evaluation metrics such as *precision* and *recall*, the proportion of true positive instances identified by the LLM relative to the total positive instances (true and false positives) and actually correct instances (true positives and false negatives), respectively. Intuitively, precision measures the model’s correctness when it makes a claim, while recall measures how much of the desired truth is actually output by the model.

8.2. Benchmarking and Evaluation Metrics

Recently, several datasets have been proposed to test the multitask accuracy of a model, across a range of academic and professional domains including mathematics, computer science, history and law [46, 86]. These benchmarks test the ability of the model to retrieve knowledge and answer reasoning tasks. Benchmarks for the chain-of-thought methodology, discussed in Subsection 7.1, which evaluate reasoning, are introduced in [90, 54] and reviewed in surveys [61, 65].

Translation tasks, introduced in Subsection 7.5, are difficult to benchmark, particularly for longer texts; availability of sufficient data for translation across multiple languages is a bottleneck in this area. We refer the reader to the discussion in [21]. The paper [93] introduces the idea of using transfer learning to enable translation between several hundred different languages, and thereby enrich the available data sets. Summarization, the subject of Subsection 7.6, is studied, for news articles, in the recent paper [113]; as for translation tasks, it is in general difficult to obtain large data sets on which to evaluate the performance of a summarization algorithm.

Recently, there has been increasing use of LLMs to evaluate other LLMs, as well as to generate text sequences for training models. This self-referential approach has clear potential drawbacks; the paper [4] illustrates these drawbacks directly in the context of using AI-generated image-data to train image-generation models.

9. Diffusion-Based Models

LLMs based on the auto-regressive factorization (3.3) currently predominate the landscape of models. However, it is entirely possible that other approaches may eventually supersede this approach. Language itself can have long-range correlations that are not necessarily well-represented by the autoregressive factorization which imposes a fixed ordering for text generation. In the setting of image generation, *diffusion-based generative modeling* has proven remarkably successful. A recently adopted line of inquiry asks how this methodology might be repurposed to generate text.

Diffusion-based generative modeling uses a forward stochastic process, defined on Euclidean space, to add noise to a data set until it is dominated by noise; reverse processes [5] may be identified which map this noise back to the data set. By learning a regularized approximation of this reverse process, a methodology may be constructed to (approximately) generate new images from the distribution underlying the data set, by initializing the reverse process from noise [85]. Choosing the forward process to be a Gaussian diffusion process (stochastic differential equation) enables efficient learning of the reverse process.

In the context of language, an alternative to sequential generation of each element of a text sequence is to predict the entire sequence (or part of a sequence) using an analog of diffusion-based generative modeling. This approach may be formulated by introducing a forward process that corrupts the entire sequence by progressively (and randomly) masking parts of it; as for diffusions, reverse processes exist which take a masked sequence back to the data distribution. Learning a regularized version of this reverse process leads to a methodology that produces an unmasked sequence drawn (approximately) from the data distribution of text sequences. This procedure is known as a *discrete diffusion model*, recognizing the fact that text sequences contain elements in a finite vocabulary V . The primary advantage of diffusion models over autoregressive models is that they generate an entire sequence at once, allowing for more efficient and sophisticated representation of causality relationships in the text sequence. The trade-off is that the reverse process requires multiple iterative steps for inference, which can have a potentially greater cost.

Recall that F^L contains sequences of length L taking values in V . For such a sequence, the total number of possible states is $|V|^L$. We now define a forward process that yields a time-indexed probability distribution $p(\cdot, t) \in \mathcal{P}(F^L)$ for $t \geq 0$. This process is initialized at the data distribution in Assumption 4.1 at $t = 0$, i.e., $p(\cdot, 0) = p_{1:L}$. The sequence of distributions then evolves according to the following continuous-time Markov chain (CTMC) [67]:

$$\frac{\partial p}{\partial t} = Qp, \quad p(\cdot, 0) = p_{1:L}. \quad (9.1)$$

The matrix-valued function of time $Q(t) \in \mathbb{R}^{|V|^L \times |V|^L}$ is known as the transition rate matrix. The matrix entries satisfy $\sum_j Q(t)_{ij} = 0$ for $i = 1, \dots, |V|^L$ [67]; this ensures that solutions $p(\cdot, t)$ defined by (9.1) indeed remain in $\mathcal{P}(F^L)$. The solution to system (9.1) defines the marginal probability of a time-indexed sequence $f_{1:L}(\cdot) : [0, T] \rightarrow F^L$ being in each state in F^L at time $t \geq 0$, starting from an initial condition $f_{1:L}(0) \sim p_{1:L}$.

Remark 9.1. Recall from Section 2.2 that we chose to simply identify each element in V with an integer in $\{1, \dots, |V|\}$. Thus we may identify the space of sequences of length L to be $\{1, \dots, |V|^L\}$. Recalling that a typical byte-pair encoded vocabulary has size $\mathcal{O}(10^4)$ (Example 2.2) and that $L = \mathcal{O}(10^4)$ for state of the art LLMs (Example 3.2) we see that the state-space of this Markov chain can be enormous. Hence, it is necessary to impose a sparse structure on $Q(\cdot)$ to define tractable numerical algorithms.

In practice, it is common to choose $Q(t) = \sigma^2(t)Q^0$ for some diffusion coefficient $\sigma(t)$ and some fixed Q^0 . That is,

$$\frac{\partial p}{\partial t} = \sigma^2(t)Q^0p. \quad (9.2)$$

If we define function $g(\cdot)$ by $g(t) = \int_0^t \sigma^2(s)ds$ and new time $\tau = g(t)$ then in terms of new time variable τ (9.2) becomes, for $p'(\tau)$ defined by $p'(g(t)) = p(t)$,

$$\frac{\partial p'}{\partial \tau} = Q^0p'. \quad (9.3)$$

If we assume that this process is ergodic so that there is a unique reference distribution $p_{\text{ref}} \in \mathcal{P}(F^L)$ with property $p'(\tau) \rightarrow p_{\text{ref}}$ as $\tau \rightarrow \infty$, and that $\sigma(\cdot)$ is such that $g \rightarrow \infty$ as $t \rightarrow \infty$, then $p(t) \rightarrow p_{\text{ref}}$ as $t \rightarrow \infty$. The following two examples present common choices for Q^0 in this setting. The two choices result, respectively, in a uniform reference distribution over F^L , or a reference distribution concentrated on a specific sequence in F^L in which each element takes value given by the same specific token (often referred to as a *mask*). In both cases we assume that $Q(t) = \sigma^2(t)Q^0$ for some diffusion coefficient $\sigma(t)$ and some fixed Q^0 chosen to obtain the desired reference distribution p_{ref} .

Example 9.2 (Uniform distribution). Consider the rate-transition matrix Q^0 defined by

$$Q_{ij}^0 = \begin{cases} 1 - \frac{|\mathcal{V}| - 1}{|\mathcal{V}|} \beta & \text{if } i = j \\ \frac{\beta}{|\mathcal{V}|} & \text{if } i \neq j \end{cases}.$$

The matrix Q^0 has any constant vector in its null-space, as required. Thus, the process in (9.1) is ergodic [67] and converges to the uniform distribution $(\mathbf{p}_{\text{ref}})_k = \frac{1}{|\mathcal{V}|}$ for $k = 1, \dots, |\mathcal{V}|$ as $t \rightarrow \infty$. By choosing large T we obtain $\mathbf{p}(\cdot; T) \approx \mathbf{p}_{\text{ref}}$.

Example 9.3 (Absorbing state). Let m represent the index of an absorbing state and consider the rate-transition matrix

$$Q_{ij}^0 = \begin{cases} 1 & \text{if } j = i = m \\ \beta & \text{if } j = m, i \neq m \\ 1 - \beta & \text{if } j \neq m, i \neq m \\ 0 & \text{otherwise} \end{cases}$$

As in the previous example, the matrix Q^0 has any constant vector in its null-space. And again the process in (9.1) is ergodic [67] and converges to the Dirac distribution $\mathbf{p}_{\text{ref}} = \delta_m$ as $t \rightarrow \infty$.

The state-space picture of the CTMC in (9.1) is a Markov process for the sequence $(f_{1:L}(t))_{t \geq 0}$ in \mathcal{F}^L that evolves continuously in time with random holding times. As a result, the process is a piecewise-constant trajectory that transitions between two states at jump times. The time between jumps is a random variable, known as the holding time, which has an exponential distribution with rate parameter $Q_{ii}(t)$ [67]. This provides the basis of numerical methods for simulating CTMCs, such as the step-by-step Gillespie algorithm [42] (that simulates each transition) and the τ -leaping algorithm [19] (that applies all transitions in a time interval at once); see [17] for application of these ideas in the context of discrete state-space diffusion models.

Given the forward process, we consider a reverse process of the form

$$\frac{\partial \bar{\mathbf{p}}}{\partial t} = \bar{Q} \bar{\mathbf{p}}, \quad \bar{\mathbf{p}}(\cdot, T) = \mathbf{p}(\cdot, T), \quad (9.4)$$

evolving backwards in time from $t = T$ to $t = 0$. Here $\bar{Q}_{ij}(t) = Q_{ji}(t) \frac{\mathbf{p}(j, t)}{\mathbf{p}(i, t)}$ is the reverse rate matrix. Then, the choice $\bar{\mathbf{p}}(\cdot, t) = \mathbf{p}(\cdot, t)$ for all $t \in [0, T]$ solves (9.4); see the proof of this result in Appendix D. In particular $\bar{\mathbf{p}}(\cdot, 0) = \mathbf{p}(\cdot, 0) = \mathbf{p}_{1:L}$. As for the forward process, we can simulate a sequence $(\bar{f}_{1:L}(t))_{t \in [0, T]}$ in \mathcal{F}^L that satisfies the reverse process. The goal of discrete diffusions is to learn the reverse rate-transition matrix \bar{Q} and simulate the reverse process to sample from the data distribution by sampling $\bar{\mathbf{p}}(\cdot, T)$. In practice \bar{Q} is known only approximately and the reverse process is initiated at $\bar{\mathbf{p}}(\cdot, T) = \mathbf{p}_{\text{ref}}$, which approximates $\mathbf{p}(\cdot, T)$. Hence the samples are only approximate samples from the desired distribution $\mathbf{p}_{1:L}$.

To define the discrete reverse process, we may learn a model for the rate transition matrix \bar{Q} using a discrete-analog of *score matching*, the methodology underlying diffusion-based image generation [85]. We also refer the reader to [17], which introduces a learning objective in discrete-time based on lower bounds for the log-likelihood of the data, and [18] for formulations based on flow matching. In [63], the authors propose to learn a network $s(\cdot, \cdot; \theta): \mathcal{F}^L \times [0, T] \rightarrow |\mathcal{V}|^L$ that approximates the probability ratios of the marginal probabilities appearing in the reverse rate matrix. That is, $s(i, t; \theta)_j \approx \frac{\mathbf{p}(j, t)}{\mathbf{p}(i, t)}$ for all pairs of inputs $i, j \in \mathcal{F}^L$. To identify s , we may minimize the loss function

$$L(\theta) := \int_0^T \mathbb{E}_{i \sim \mathbf{p}(\cdot, t)} \left[\sum_{j \neq i} s(i, t; \theta)_j - \frac{\mathbf{p}(j, t)}{\mathbf{p}(i, t)} \log s(i, t; \theta)_j \right] dt.$$

Given that $s \mapsto s - \alpha \log s$ is minimized at $s = \alpha$ we have that L is minimized at the desired probability ratio. Moreover, by the tower rule, the loss can be equivalently written in terms of the conditional distributions, which are specified by the marginal forward process in (9.1) and hence known. That is,

$$\mathsf{L}(\theta) = \int_0^T \mathbb{E}_{i \sim \mathbf{p}(\cdot, t|k), k \sim \mathbf{p}_{1:L}} \left[\sum_{j \neq i} \mathbf{s}(i, t; \theta)_j - \frac{\mathbf{p}(j, t|k)}{\mathbf{p}(i, t|k)} \log \mathbf{s}(i, t; \theta)_j \right] dt.$$

This loss is implementable given samples from the data distribution and yields an estimator for the reverse rate matrix, which can be used to generate new samples by evolving the reverse process in (9.4) with this approximate rate. That is, by evolving $\bar{f}(t)$ backwards-in-time starting from $\bar{f}(T) \sim \mathbf{p}_{\text{ref}}$ to $t = 0$ according to the CTMC with the rate matrix whose entries are given by

$$\bar{Q}_{ij}(t) = Q_{ji}(t) \mathbf{s}(i, t; \theta)_j, \quad (9.5)$$

for all i, j . The resulting sequence $\bar{f}(0)$ is an approximate sample from $\mathbf{p}_{1:L}$.

10. Summary and Challenges

Text Encoding in Euclidean Space: In Remark 2.5 and Example 3.2 we highlight the trade-off between vocabulary size and sequence length. The question of how to optimally balance this trade-off will depend on the details of the LLM architecture. Current algorithms simply demonstrate empirical success with the use of byte-pair encoding. Analysis of this trade-off has the potential to guide new architectural developments, linked to concepts from information theory. Relatedly, the question of how to embed sequences in \mathbf{V} as sequences in \mathbf{V}_e leaves open many natural questions, alluded to in Remark 2.9: what is the optimal choice of dimension d_e ? Do LLMs automatically learn an embedding for text sequences that has semantic meaning and how does regularity in the embedding space affect the resulting model learning problems?

Long Context Length: As mentioned in Subsection 7.3, prompts which contain substantial information (context) are used to avoid fine-tuning of LLMs and adapt the model to specific tasks. However, the computational complexity of next-token prediction models for long sequence generation creates a bottleneck in this approach. This has motivated new methodologies that can compress long sequences. One such methodology replaces commonplace fragments of sequences using GIST tokens [66, 69]. Another constraint in most practical LLMs is the maximum context length. For example, the diffusion processes in Section 9 set this length in advance and sample sequences of fixed length. It is of interest to develop approaches that can operate across different dimensional spaces, and which can adjust the maximum context length based on each task.

Robustness: LLMs have been shown to result in wide variety of responses under adversarial perturbations to their inputs [106, 117]; this has potential to affect their safe development and public trust in the technology. In particular, quite reasonable text prompts can lead to *hallucinations*: generated content which is factually incorrect or nonsensical. An important direction for study is to investigate the sensitivity of the next-token probability model, and the resulting semantic meaning of the generated output, to various perturbations in the model. These might include the input context, model parameters and fine-tuning. This will be useful for designing architectures whose output is more robust to certain perturbations.

Optimal Use Of Data: Remark 4.7 discusses the fact that typically the desired population level objective function is approximated in a biased way, using correlated data samples. A statistical evaluation of this finite-sample estimator, in comparison with unbiased ample-based approximation, is an interesting research direction. More generally, there are several interesting questions about the trade-off between accuracy and computational complexity in the use of data. Another example is in the decomposition of data to enable it to fit into the context window; what is the optimal way to break up and use the data?

Scaling Laws: Recent empirical studies show that the accuracy of LLMs (as measured using various metrics, see Section 8) follow seemingly deterministic power-law relationships with increasing model parameters, the volume of training data, and the amount of computational resources (FLOPs) [56, 47]. These trends are often used to inform economic decisions by predicting the performance of models under different training configurations; for example to assess whether training a larger model on more data is cost-effective. However, scaling laws fit simple functional forms to historical training data and assume that power-laws extrapolate to new model settings. Developing mechanistic models that explain these trends by accounting for different architectures, variations in dataset quality, and changing parameters in optimization algorithms with quantified uncertainty will underpin these empirical studies, and yield scaling laws that extrapolate more reliably.

Synthetic Data and Watermarking: With the increasing amount of human-generated data being used for training (see Remark 4.2), there is growing possibility that models will be trained on synthetic data that has been generated by another model. This behavior can lead to a degradation in the quality of the generated samples and a bias relative to the true data distribution, a phenomenon referred to as *mode collapse* [84, 4]. To avoid this, *watermarking* is used, an approach to embed a signal in the generated text that can be used to detect LLM-generated data [58]. Such data can be excluded from fine-tuning, or can be weighted differently from naturally occurring data; research is needed to understand how best to do this.

Test-Time Reasoning: In Subsection 7.1 we discussed the Chain-of-Thought approach to making reasoning explicit via prompting. A related emerging approach is *test-time reasoning* (also known as test-time scaling or thinking). This refers to devoting appreciable computing resources at inference-time to improve the correctness of the model’s predictions on hard tasks. In several modern deployments, this is achieved through interaction of the model with the user by generating intermediate tokens (sometimes hidden, sometimes shown) before committing to an answer. The value of the trade-off between latency/cost of this procedure and its reliability will depend on the task. Algorithmic approaches for test-time reasoning include eliciting longer chains-of-thought [103], sampling multiple reasoning paths and selecting a subset of them for consistency [100], and more explicit search over thought states, for example via Tree/Forest-of-Thought methods [107]. Mathematically, a natural perspective is to treat thoughts as latent variables. Test-time reasoning may then be viewed as a form of budget-constrained inference with the goal of maximizing an evaluation metric; see Section 8. For example, we can optimize over trajectories to shift the model’s output distribution toward more globally consistent responses. Deeper understanding of this process has the potential to create more effective algorithms.

Acknowledgments

The work of AMS is partially supported by a Department of Defense (DoD) Vannevar Bush Faculty Fellowship (award N00014-22-1-2790).

References

- [1] ABDIN, M., ANEJA, J., BEHL, H., BUBECK, S., ELDAN, R., GUNASEKAR, S., HARRISON, M., HEWETT, R. J., JAVAHERIPI, M., KAUFFMANN, P. et al. (2024). Phi-4 technical report. *arXiv preprint arXiv:2412.08905*.
- [2] ACHIAM, J., ADLER, S., AGARWAL, S., AHMAD, L., AKKAYA, I., ALEMAN, F. L., ALMEIDA, D., ALTENSCHMIDT, J., ALTMAN, S., ANADKAT, S. et al. (2023). GPT-4 technical report. *arXiv preprint arXiv:2303.08774*.
- [3] ADAM, K. D. B. J. et al. (2014). A method for stochastic optimization. *arXiv preprint arXiv:1412.6980* **1412**.
- [4] ALEMOHAMMAD, S., CASCO-RODRIGUEZ, J., LUZI, L., HUMAYUN, A. I., BABAEI, H., LEJEUNE, D., SIAHKOOHI, A. and BARANIUK, R. (2024). Self-Consuming Generative Models Go MAD. In *The Twelfth International Conference on Learning Representations*.
- [5] ANDERSON, B. D. (1982). Reverse-time diffusion equation models. *Stochastic Processes and their Applications* **12** 313–326.
- [6] ANSARI, A. F., STELLA, L., TURKMEN, C., ZHANG, X., MERCADO, P., SHEN, H., SHCHUR, O., RANGAPURAM, S. S., ARANGO, S. P., KAPOOR, S. et al. (2024). Chronos: Learning the language of time series. *arXiv preprint arXiv:2403.07815*.
- [7] ANTHROPIC (2025). Claude 4 Family: Opus, Sonnet, and Haiku Models. <https://www.anthropic.com/index/clause-4>. Accessed: 2025-07-29.
- [8] AUSTIN, J., JOHNSON, D. D., HO, J., TARLOW, D. and VAN DEN BERG, R. (2021). Structured denoising diffusion models in discrete state-spaces. *Advances in neural information processing systems* **34** 17981–17993.
- [9] AZAR, M. G., GUO, Z. D., PIOT, B., MUNOS, R., ROWLAND, M., VALKO, M. and CALANDRIELLO, D. (2024). A general theoretical paradigm to understand learning from human preferences. In *International Conference on Artificial Intelligence and Statistics* 4447–4455. PMLR.
- [10] BA, J. L., KIROS, J. R. and HINTON, G. E. (2016). Layer normalization. *arXiv preprint arXiv:1607.06450*.
- [11] BACH, E., BAPTISTA, R., CALVELLO, E., CHEN, B. and STUART, A. (2025). Learning Enhanced Ensemble Filters. *arXiv preprint arXiv:2504.17836*.
- [12] BACH, E., BAPTISTA, R., SANZ-ALONSO, D. and STUART, A. (2024). Machine Learning for Inverse Problems and Data Assimilation. *arXiv preprint arXiv:2410.10523*.
- [13] BACHMANN, R., KAR, O. F., MIZRAHI, D., GARJANI, A., GAO, M., GRIFFITHS, D., HU, J., DEHGHAN, A. and ZAMIR, A. (2024). 4M-21: An any-to-any vision model for tens of tasks and modalities. *Advances in Neural Information Processing Systems* **37** 61872–61911.
- [14] BAPTISTA, R., STUART, A. M. and TRAN, S. (2025). A Mathematical Perspective On Contrastive Learning. *arXiv preprint arXiv:2505.24134*.
- [15] BROWN, T., MANN, B., RYDER, N., SUBBIAH, M., KAPLAN, J. D., DHARIWAL, P., NEE-LAKANTAN, A., SHYAM, P., SASTRY, G., ASKELL, A. et al. (2020). Language models are few-shot learners. *Advances in neural information processing systems* **33** 1877–1901.
- [16] CALVELLO, E., KOVACHKI, N. B., LEVINE, M. E. and STUART, A. M. (2024). Continuum attention for neural operators. *arXiv preprint arXiv:2406.06486*.
- [17] CAMPBELL, A., BENTON, J., DE BORTOLI, V., RAINFORTH, T., DELIGIANNIDIS, G. and DOUCET, A. (2022). A continuous time framework for discrete denoising models. *Advances in Neural Information Processing Systems* **35** 28266–28279.
- [18] CAMPBELL, A., YIM, J., BARZILAY, R., RAINFORTH, T. and JAAKKOLA, T. (2024). Generative Flows on Discrete State-Spaces: Enabling Multimodal Flows with Applications to Protein

Co-Design. In *International Conference on Machine Learning* 5453–5512. PMLR.

[19] CAO, Y., GILLESPIE, D. T. and PETZOLD, L. R. (2006). Efficient step size selection for the tau-leaping simulation method. *The Journal of chemical physics* **124**.

[20] CASTIN, V., ABLIN, P., CARRILLO, J. A. and PEYRÉ, G. (2025). A unified perspective on the dynamics of deep transformers. *arXiv preprint arXiv:2501.18322*.

[21] CHAUHAN, S. and DANIEL, P. (2023). A comprehensive survey on various fully automatic machine translation evaluation metrics. *Neural Processing Letters* **55** 12663–12717.

[22] CHEN, J., PAN, X., YU, D., SONG, K., WANG, X., YU, D. and CHEN, J. (2023). Skills-in-context prompting: Unlocking compositionality in large language models. *arXiv preprint arXiv:2308.00304*.

[23] CHEN, L., LU, K., RAJESWARAN, A., LEE, K., GROVER, A., LASKIN, M., ABBEEL, P., SRINIVAS, A. and MORDATCH, I. (2021). Decision transformer: Reinforcement learning via sequence modeling. *Advances in neural information processing systems* **34** 15084–15097.

[24] CHEN, S., LIN, Z., POLYANSKIY, Y. and RIGOLLET, P. (2025). Quantitative Clustering in Mean-Field Transformer Models. *arXiv preprint arXiv:2504.14697*.

[25] CHILD, R., GRAY, S., RADFORD, A. and SUTSKEVER, I. (2019). Generating long sequences with sparse transformers. *arXiv preprint arXiv:1904.10509*.

[26] CHOROMANSKI, K., LIKHOSHERSTOV, V., DOHAN, D., SONG, X., GANE, A., SARLOS, T., HAWKINS, P., DAVIS, J., MOHIUDDIN, A., KAISER, L. et al. (2020). Rethinking attention with performers. *arXiv preprint arXiv:2009.14794*.

[27] CHRISTIANO, P. F., LEIKE, J., BROWN, T., MARTIC, M., LEGG, S. and AMODEI, D. (2017). Deep reinforcement learning from human preferences. *Advances in neural information processing systems* **30**.

[28] D’ANGELO, F., ANDRIUSHCHENKO, M., VARRE, A. V. and FLAMMARION, N. (2024). Why do we need weight decay in modern deep learning? *Advances in Neural Information Processing Systems* **37** 23191–23223.

[29] DAO, T., FU, D., ERMON, S., RUDRA, A. and RÉ, C. (2022). FlashAttention: Fast and memory-efficient exact attention with IO-awareness. *Advances in neural information processing systems* **35** 16344–16359.

[30] DING, H., WANG, Z., PAOLINI, G., KUMAR, V., DEORAS, A., ROTH, D. and SOATTO, S. (2024). Fewer truncations improve language modeling. *arXiv preprint arXiv:2404.10830*.

[31] DONOHO, D. (2024). Data science at the singularity. *Harvard Data Science Review* **6**.

[32] DOSOVITSKIY, A., BEYER, L., KOLESNIKOV, A., WEISSENBORN, D., ZHAI, X., UNTERHINER, T., DEHGHANI, M., MINDERER, M., HEIGOLD, G., GELLY, S. et al. (2020). An Image is Worth 16x16 Words: Transformers for Image Recognition at Scale. In *International Conference on Learning Representations*.

[33] ENGL, H., HANKE, M. and NEUBAUER, A. (1996). Regularization of Inverse Problems. *Kluwer Academic Publishers; Dordrecht, Boston, London*.

[34] FREITAG, M. and AL-ONAIZAN, Y. (2017). Beam Search Strategies for Neural Machine Translation. In *Proceedings of the First Workshop on Neural Machine Translation* 56–60.

[35] FRIEDER, S., BERNER, J., PETERSEN, P. and LUKASIEWICZ, T. (2023). Large language models for mathematicians. *arXiv preprint arXiv:2312.04556*.

[36] GAGE, P. (1994). A new algorithm for data compression. *The C Users Journal* **12** 23–38.

[37] GERSTGRASSER, M., SCHAEFFER, R., DEY, A., RAFAILOV, R., SLEIGHT, H., HUGHES, J., KORBAK, T., AGRAWAL, R., PAI, D., GROMOV, A. et al. (2024). Is model collapse inevitable? breaking the curse of recursion by accumulating real and synthetic data. *arXiv preprint arXiv:2404.01413*.

[38] GESHKOVSKI, B., KOUBBI, H., POLYANSKIY, Y. and RIGOLLET, P. (2024). Dynamic metasta-

bility in the self-attention model. *arXiv preprint arXiv:2410.06833*.

[39] GESHKOVSKI, B., LETROUIT, C., POLYANSKIY, Y. and RIGOLLET, P. (2023). The emergence of clusters in self-attention dynamics. *Advances in Neural Information Processing Systems* **36** 57026–57037.

[40] GESHKOVSKI, B., LETROUIT, C., POLYANSKIY, Y. and RIGOLLET, P. (2025). A mathematical perspective on transformers. *Bulletin of the American Mathematical Society* **62** 427–479.

[41] GESHKOVSKI, B., RIGOLLET, P. and RUIZ-BALET, D. (2024). Measure-to-measure interpolation using Transformers. *arXiv preprint arXiv:2411.04551*.

[42] GILLESPIE, D. T. (1977). Exact stochastic simulation of coupled chemical reactions. *The journal of physical chemistry* **81** 2340–2361.

[43] GOODFELLOW, I., BENGIO, Y., COURVILLE, A. and BENGIO, Y. (2016). *Deep Learning* **1**. MIT press Cambridge.

[44] GRATTAFIORI, A., DUBEY, A., JAURHI, A., PANDEY, A., KADIAN, A., AL-DAHLE, A., LETMAN, A., MATHUR, A., SCHELTON, A., VAUGHAN, A. et al. (2024). The Llama 3 herd of models. *arXiv preprint arXiv:2407.21783*.

[45] GUU, K., LEE, K., TUNG, Z., PASUPAT, P. and CHANG, M. (2020). Retrieval augmented language model pre-training. In *International conference on machine learning* 3929–3938. PMLR.

[46] HENDRYCKS, D., BURNS, C., BASART, S., ZOU, A., MAZEIKA, M., SONG, D. and STEINHARDT, J. (2020). Measuring massive multitask language understanding. *arXiv preprint arXiv:2009.03300*.

[47] HOFFMANN, J., BORGEAUD, S., MENSCH, A., BUCHATSKAYA, E., CAI, T., RUTHERFORD, E., DE LAS CASAS, D., HENDRICKS, L. A., WELBL, J., CLARK, A. et al. (2022). Training compute-optimal large language models. In *Proceedings of the 36th International Conference on Neural Information Processing Systems* 30016–30030.

[48] HOLTZMAN, A., BUYS, J., DU, L., FORBES, M. and CHOI, Y. (2020). The Curious Case of Neural Text Degeneration. In *International Conference on Learning Representations*.

[49] HOOGEBOOM, E., NIELSEN, D., JAINI, P., FORRÉ, P. and WELLING, M. (2021). Argmax flows and multinomial diffusion: Learning categorical distributions. *Advances in neural information processing systems* **34** 12454–12465.

[50] HU, E. J., SHEN, Y., WALLIS, P., ALLEN-ZHU, Z., LI, Y., WANG, S., WANG, L., CHEN, W. et al. (2022). LoRA: Low-rank adaptation of large language models. In *International Conference on Learning Representations* **1** 3.

[51] HU, K., GAO, F., NIE, X., ZHOU, P., TRAN, S., NEIMAN, T., WANG, L., SHAH, M., HAMID, R., YIN, B. et al. (2025). M-LLM based video frame selection for efficient video understanding. In *Proceedings of the Computer Vision and Pattern Recognition Conference* 13702–13712.

[52] HUI, B., YANG, J., CUI, Z., YANG, J., LIU, D., ZHANG, L., LIU, T., ZHANG, J., YU, B., LU, K. et al. (2024). Qwen2. 5-coder technical report. *arXiv preprint arXiv:2409.12186*.

[53] COHERE INC. (2025). A Guide to Tokens and Tokenizers. <https://docs.cohere.com/v2/docs/tokens-and-tokenizers>. Accessed: 2025-09-23.

[54] JIANG, D., ZHANG, R., GUO, Z., LI, Y., QI, Y., CHEN, X., WANG, L., JIN, J., GUO, C., YAN, S. et al. (2025). MME-CoT: Benchmarking chain-of-thought in large multimodal models for reasoning quality, robustness, and efficiency. *arXiv preprint arXiv:2502.09621*.

[55] JUMPER, J., EVANS, R., PRITZEL, A., GREEN, T., FIGURNOV, M., RONNEBERGER, O., TUNYASUVUNAKOOL, K., BATES, R., ŽÍDEK, A., POTAPENKO, A. et al. (2021). Highly accurate protein structure prediction with AlphaFold. *nature* **596** 583–589.

[56] KAPLAN, J., MCCANDLISH, S., HENIGHAN, T., BROWN, T. B., CHESS, B., CHILD, R.,

GRAY, S., RADFORD, A., WU, J. and AMODEI, D. (2020). Scaling laws for neural language models. *arXiv preprint arXiv:2001.08361*.

[57] KARAGODIN, N., POLYANSKIY, Y. and RIGOLLET, P. (2024). Clustering in causal attention masking. *Advances in Neural Information Processing Systems* **37** 115652–115681.

[58] KIRCHENBAUER, J., GEIPING, J., WEN, Y., KATZ, J., MIERS, I. and GOLDSTEIN, T. (2023). A watermark for large language models. In *International Conference on Machine Learning* 17061–17084. PMLR.

[59] KOBAYASHI, S., AKRAM, Y. and VON OSWALD, J. (2024). Weight decay induces low-rank attention layers. *Advances in Neural Information Processing Systems* **37** 4481–4510.

[60] LECUN, Y., BOTTOU, L., BENGIO, Y. and HAFFNER, P. (2002). Gradient-based learning applied to document recognition. *Proceedings of the IEEE* **86** 2278–2324.

[61] LEE, J. and HOCKENMAIER, J. (2025). Evaluating Step-by-step Reasoning Traces: A Survey. *CoRR* **abs/2502.12289**.

[62] LEWIS, P., PEREZ, E., PIKTUS, A., PETRONI, F., KARPUKHIN, V., GOYAL, N., KÜTTLER, H., LEWIS, M., YIH, W.-T., ROCKTÄSCHEL, T. et al. (2020). Retrieval-augmented generation for knowledge-intensive NLP tasks. *Advances in neural information processing systems* **33** 9459–9474.

[63] LOU, A., MENG, C. and ERMON, S. (2024). Discrete diffusion modeling by estimating the ratios of the data distribution. In *Proceedings of the 41st International Conference on Machine Learning* 32819–32848.

[64] MIZRAHI, D., BACHMANN, R., KAR, O., YEO, T., GAO, M., DEHGHAN, A. and ZAMIR, A. (2023). 4M: Massively multimodal masked modeling. *Advances in Neural Information Processing Systems* **36** 58363–58408.

[65] MONDORF, P. and PLANK, B. (2024). Beyond Accuracy: Evaluating the Reasoning Behavior of Large Language Models - A Survey. In *First Conference on Language Modeling*.

[66] MU, J., LI, X. and GOODMAN, N. (2023). Learning to compress prompts with gist tokens. *Advances in Neural Information Processing Systems* **36** 19327–19352.

[67] NORRIS, J. R. (1998). *Markov chains* **2**. Cambridge university press.

[68] OUYANG, L., WU, J., JIANG, X., ALMEIDA, D., WAINWRIGHT, C., MISHKIN, P., ZHANG, C., AGARWAL, S., SLAMA, K., RAY, A. et al. (2022). Training language models to follow instructions with human feedback. *Advances in neural information processing systems* **35** 27730–27744.

[69] PETROV, A., SANDLER, M., ZHMOGINOV, A., MILLER, N. and VLADYMYROV, M. (2025). Long Context In-Context Compression by Getting to the Gist of Gisting. *arXiv preprint arXiv:2504.08934*.

[70] PHUONG, M. and HUTTER, M. (2022). Formal algorithms for transformers. *arXiv preprint arXiv:2207.09238*.

[71] RADFORD, A., KIM, J. W., HALLACY, C., RAMESH, A., GOH, G., AGARWAL, S., SASTRY, G., ASKELL, A., MISHKIN, P., CLARK, J. et al. (2021). Learning transferable visual models from natural language supervision. In *International conference on machine learning* 8748–8763. PMLR.

[72] RADFORD, A., METZ, L. and CHINTALA, S. (2015). Unsupervised representation learning with deep convolutional generative adversarial networks. *arXiv preprint arXiv:1511.06434*.

[73] RADFORD, A., WU, J., CHILD, R., LUAN, D., AMODEI, D., SUTSKEVER, I. et al. (2019). Language models are unsupervised multitask learners. *OpenAI blog* **1** 9.

[74] RAFAILOV, R., SHARMA, A., MITCHELL, E., MANNING, C. D., ERMON, S. and FINN, C. (2023). Direct preference optimization: Your language model is secretly a reward model. *Advances in neural information processing systems* **36** 53728–53741.

[75] RAFFEL, C., SHAZER, N., ROBERTS, A., LEE, K., NARANG, S., MATENA, M., ZHOU, Y.,

LI, W. and LIU, P. J. (2020). Exploring the limits of transfer learning with a unified text-to-text transformer. *Journal of Machine Learning Research* **21** 1–67.

[76] RAJARAMAN, N., JIAO, J. and RAMCHANDRAN, K. (2024). Toward a theory of tokenization in LLMs. *arXiv preprint arXiv:2404.08335*.

[77] RAZAVI, A., VAN DEN OORD, A. and VINYALS, O. (2019). Generating diverse high-fidelity images with VQ-VAE-2. *Advances in Neural Information Processing Systems* **32**.

[78] ROBBINS, H. and MONRO, S. (1951). A stochastic approximation method. *The annals of mathematical statistics* 400–407.

[79] SAHOO, S., ARRIOLA, M., SCHIFF, Y., GOKASLAN, A., MARROQUIN, E., CHIU, J., RUSH, A. and KULESHOV, V. (2024). Simple and effective masked diffusion language models. *Advances in Neural Information Processing Systems* **37** 130136–130184.

[80] SENNICH, R., HADDOW, B. and BIRCH, A. (2016). Neural Machine Translation of Rare Words with Subword Units. In *Proceedings of the 54th Annual Meeting of the Association for Computational Linguistics (Volume 1: Long Papers)* (K. ERK and N. A. SMITH, eds.) 1715–1725. Association for Computational Linguistics, Berlin, Germany.

[81] SHANNON, C. E. (1948). A mathematical theory of communication. *The Bell system technical journal* **27** 379–423.

[82] SHAO, Z., WANG, P., ZHU, Q., XU, R., SONG, J., BI, X., ZHANG, H., ZHANG, M., LI, Y., WU, Y. et al. (2024). Deepseekmath: Pushing the limits of mathematical reasoning in open language models. *arXiv preprint arXiv:2402.03300*.

[83] SHI, J., HAN, K., WANG, Z., DOUCET, A. and TITSIAS, M. (2024). Simplified and generalized masked diffusion for discrete data. *Advances in neural information processing systems* **37** 103131–103167.

[84] SHUMAILOV, I., SHUMAYLOV, Z., ZHAO, Y., PAPERNOT, N., ANDERSON, R. and GAL, Y. (2024). AI models collapse when trained on recursively generated data. *Nature* **631** 755–759.

[85] SONG, Y., SOHL-DICKSTEIN, J., KINGMA, D. P., KUMAR, A., ERMON, S. and POOLE, B. (2021). Score-based generative modeling through stochastic differential equations. In *International Conference on Learning Representations*.

[86] SRIVASTAVA, A., RASTOGI, A., RAO, A., SHOEB, A. A. M., ABID, A., FISCH, A., BROWN, A. R., SANTORO, A., GUPTA, A., GARRIGA-ALONSO, A. et al. (2023). Beyond the imitation game: Quantifying and extrapolating the capabilities of language models. *Transactions on machine learning research*.

[87] STIENNEN, N., OUYANG, L., WU, J., ZIEGLER, D., LOWE, R., VOSS, C., RADFORD, A., AMODEI, D. and CHRISTIANO, P. F. (2020). Learning to summarize with human feedback. *Advances in neural information processing systems* **33** 3008–3021.

[88] SU, J., AHMED, M., LU, Y., PAN, S., BO, W. and LIU, Y. (2024). RoFormer: Enhanced transformer with rotary position embedding. *Neurocomputing* **568** 127063.

[89] SUN, Q., CUI, Y., ZHANG, X., ZHANG, F., YU, Q., WANG, Y., RAO, Y., LIU, J., HUANG, T. and WANG, X. (2024). Generative multimodal models are in-context learners. In *Proceedings of the IEEE/CVF Conference on Computer Vision and Pattern Recognition* 14398–14409.

[90] SUZGUN, M., SCALES, N., SCHÄRLI, N., GEHRMANN, S., TAY, Y., CHUNG, H. W., CHOWDHERY, A., LE, Q., CHI, E., ZHOU, D. et al. (2023). Challenging big-bench tasks and whether chain-of-thought can solve them. In *Findings of the Association for Computational Linguistics: ACL 2023* 13003–13051.

[91] TEAM, G., ANIL, R., BORGEAUD, S., ALAYRAC, J.-B., YU, J., SORICUT, R., SCHALKWYK, J., DAI, A. M., HAUTH, A., MILLICAN, K. et al. (2023). Gemini: a family of highly capable multimodal models. *arXiv preprint arXiv:2312.11805*.

[92] TEAM, K., ZHANG, Y., LIN, Z., YAO, X., HU, J., MENG, F., LIU, C., MEN, X., YANG, S.,

LI, Z. et al. (2025). Kimi Linear: An Expressive, Efficient Attention Architecture. *arXiv preprint arXiv:2510.26692*.

[93] TEAM, N. (2024). Scaling neural machine translation to 200 languages. *Nature* **630** 841–846.

[94] THE MATHWORKS, INC. (2025). Choose an ODE Solver — MATLAB & Simulink. <https://www.mathworks.com/help/matlab/math/choose-an-ode-solver.html>. Accessed: 2025-11-05.

[95] TOUVRON, H., LAVRIL, T., IZACARD, G., MARTINET, X., LACHAUX, M.-A., LACROIX, T., ROZIÈRE, B., GOYAL, N., HAMBRO, E., AZHAR, F. et al. (2023). LLaMA: Open and efficient foundation language models. *arXiv preprint arXiv:2302.13971*.

[96] TURNER, R. E. (2023). An introduction to transformers. *arXiv preprint arXiv:2304.10557*.

[97] VASWANI, A., SHAZER, N., PARMAR, N., USZKOREIT, J., JONES, L., GOMEZ, A. N., KAISER, L. U. and POLOSUKHIN, I. (2017). Attention is all you need. In *Advances in Neural Information Processing Systems* (I. GUYON, U. V. LUXBURG, S. BENGIO, H. WALLACH, R. FERGUS, S. VISHWANATHAN and R. GARNETT, eds.) **30**. Curran Associates, Inc.

[98] VILLALOBOS, P., HO, A., SEVILLA, J., BESIROGLU, T., HEIM, L. and HOBBHAHN, M. (2022). Will we run out of data? Limits of LLM scaling based on human-generated data. *arXiv preprint arXiv:2211.04325*.

[99] WAN, Z. Y., BAPTISTA, R., BORAL, A., CHEN, Y.-F., ANDERSON, J., SHA, F. and ZEPEDA-NÚÑEZ, L. (2023). Debias coarsely, sample conditionally: Statistical downscaling through optimal transport and probabilistic diffusion models. *Advances in Neural Information Processing Systems* **36** 47749–47763.

[100] WANG, X., WEI, J., SCHUURMANS, D., LE, Q., CHI, E., NARANG, S., CHOWDHERY, A. and ZHOU, D. (2022). Self-consistency improves chain of thought reasoning in language models. *arXiv preprint arXiv:2203.11171*.

[101] WANG, X., WEI, J., SCHUURMANS, D., LE, Q. V., CHI, E. H., NARANG, S., CHOWDHERY, A. and ZHOU, D. (2023). Self-Consistency Improves Chain of Thought Reasoning in Language Models. In *The Eleventh International Conference on Learning Representations*.

[102] WANG, X. and ZHOU, D. (2024). Chain-of-thought reasoning without prompting. *Advances in Neural Information Processing Systems* **37** 66383–66409.

[103] WEI, J., WANG, X., SCHUURMANS, D., BOSMA, M., XIA, F., CHI, E., LE, Q. V., ZHOU, D. et al. (2022). Chain-of-thought prompting elicits reasoning in large language models. *Advances in neural information processing systems* **35** 24824–24837.

[104] WU, S., FEI, H., QU, L., JI, W. and CHUA, T.-S. (2024). Next-GPT: Any-to-any multimodal LLM. In *Forty-first International Conference on Machine Learning*.

[105] XIONG, R., YANG, Y., HE, D., ZHENG, K., ZHENG, S., XING, C., ZHANG, H., LAN, Y., WANG, L. and LIU, T. (2020). On layer normalization in the transformer architecture. In *International conference on machine learning* 10524–10533. PMLR.

[106] XU, X., KONG, K., LIU, N., CUI, L., WANG, D., ZHANG, J. and KANKANHALLI, M. (2023). An LLM can fool itself: A prompt-based adversarial attack. *arXiv preprint arXiv:2310.13345*.

[107] YAO, S., YU, D., ZHAO, J., SHAFRAN, I., GRIFFITHS, T. L., CAO, Y. and NARASIMHAN, K. (2023). Tree of thoughts: Deliberate problem solving with large language models, 2023. *URL https://arxiv.org/abs/2305.10601* **3** 1.

[108] ZEHUI, L., LIU, P., HUANG, L., CHEN, J., QIU, X. and HUANG, X. (2019). DropAttention: A regularization method for fully-connected self-attention networks. *arXiv preprint arXiv:1907.11065*.

[109] ZHAN, J., DAI, J., YE, J., ZHOU, Y., ZHANG, D., LIU, Z., ZHANG, X., YUAN, R., ZHANG, G., LI, L. et al. (2024). AnyGPT: Unified multimodal LLM with discrete sequence modeling. *arXiv preprint arXiv:2402.12226*.

- [110] ZHANG, B. and SENNICH, R. (2019). Root mean square layer normalization. *Advances in neural information processing systems* **32**.
- [111] ZHANG, J., ZHAO, Y., SALEH, M. and LIU, P. (2020). Pegasus: Pre-training with extracted gap-sentences for abstractive summarization. In *International conference on machine learning* 11328–11339. PMLR.
- [112] ZHANG, R., ZHAI, S., GU, J., ZHANG, Y., ZHENG, H., CHEN, T., BAUTISTA, M. A., SUSSKIND, J. and JAITLEY, N. (2025). Flexible Language Modeling in Continuous Space with Transformer-based Autoregressive Flows. *arXiv preprint arXiv:2507.00425*.
- [113] ZHANG, T., LADHAK, F., DURMUS, E., LIANG, P., MCKEOWN, K. and HASHIMOTO, T. B. (2024). Benchmarking large language models for news summarization. *Transactions of the Association for Computational Linguistics* **12** 39–57.
- [114] ZHAO, W. X., ZHOU, K., LI, J., TANG, T., WANG, X., HOU, Y., MIN, Y., ZHANG, B., ZHANG, J., DONG, Z. et al. (2023). A survey of large language models. *arXiv preprint arXiv:2303.18223*.
- [115] ZHOU, W., GE, T., WEI, F., ZHOU, M. and XU, K. (2020). Scheduled DropHead: A Regularization Method for Transformer Models. In *Findings of the Association for Computational Linguistics: EMNLP 2020* 1971–1980.
- [116] ZHU, J., CHEN, X., HE, K., LECUN, Y. and LIU, Z. (2025). Transformers without normalization. In *Proceedings of the Computer Vision and Pattern Recognition Conference* 14901–14911.
- [117] ZHU, K., WANG, J., ZHOU, J., WANG, Z., CHEN, H., WANG, Y., YANG, L., YE, W., ZHANG, Y., GONG, N. et al. (2023). PromptRobust: Towards evaluating the robustness of large language models on adversarial prompts. In *Proceedings of the 1st ACM workshop on large AI systems and models with privacy and safety analysis* 57–68.
- [118] ZIEGLER, D. M., STIENNEN, N., WU, J., BROWN, T. B., RADFORD, A., AMODEI, D., CHRISTIANO, P. and IRVING, G. (2019). Fine-tuning language models from human preferences. *arXiv preprint arXiv:1909.08593*.
- [119] ZIV, J. and LEMPEL, A. (2003). A universal algorithm for sequential data compression. *IEEE Transactions on information theory* **23** 337–343.

Appendix A: Derivatives

The next-token probability model defined in (5.1) is parameterized by $\theta = (\vartheta, \varphi)$. The objective function $L^N(\theta)$, given in (4.5), is minimized using gradient descent-based methods; thus we need to be able to differentiate the model with respect to both ϑ and φ . The following two subsections describe some details relating to the computation of these derivatives, details that are useful to understand how gradient-based training is implemented. The derivatives are also useful beyond training, for example, to understand the sensitivity of the trained model to perturbations of its inputs.

A.1. φ Derivative

Recall the approximation (5.1) for the learnable probability distribution on sequences in token-space, noting that it is built from $q_m(\cdot | \cdot; \vartheta) : F_e^{(m-1)} \rightarrow \mathcal{P}(V)$. Sequences in $F_e^{(m-1)}$ (Euclidean space valued) are constructed from sequences in $F^{(m-1)}$ (token space valued) by application of map ϕ defined by parameter $\varphi \in \mathbb{R}^{d_e \times |V|}$. In particular, $h \in F_e^{(m-1)}$ is found from $f \in F^{(m-1)}$ via $h = \phi \circ f$. We describe how to differentiate q_m with respect to this dependence on φ . Noting that $\mathcal{P}(V) \subset \mathbb{R}^{|V|}$,

we abstract this question to consider differentiating maps from $\mathbb{R}^{d_e \times |\mathcal{V}|} \times \mathcal{F}^M$ into $\mathbb{R}^{|\mathcal{V}|}$ with respect to their first argument.

We have chosen to label the elements in vocabulary \mathcal{V} by making the identification $\mathcal{V} = \{1, \dots, |\mathcal{V}|\} = \mathbb{S}^{|\mathcal{V}|}$. Recall also, from Definition 2.6, that $\phi : \mathcal{V} \rightarrow \mathbb{R}^{d_e}$ is defined by matrix

$$\varphi \in \mathbb{R}^{d_e \times |\mathcal{V}|}, \quad \varphi = (\theta_1, \dots, \theta_{|\mathcal{V}|}), \quad \theta_m \in \mathbb{R}^{d_e}$$

where $\theta_m \in \mathbb{R}^{d_e}$ for all $m \in \mathcal{V}$; then $\phi(v) = \theta_v$. Definition 2.7 extends ϕ to act on sequences: for sequence $f \in \mathcal{F}^M$, sequence $h = \phi \circ f \in \mathcal{F}_e^M$ is given by

$$h = (h_1, \dots, h_M) \in \mathcal{F}_e^M, \quad h_m = \phi(f_m) \in \mathbb{R}^{d_e}.$$

Now assume that we are given function $\mathbf{G} : \mathcal{F}_e^M \rightarrow \mathbb{R}^{|\mathcal{V}|}$ and let $D_m \mathbf{G}(h) = \partial_{h_m} \mathbf{G}(h)$. Note that, for every $h \in \mathcal{F}_e^M$, $D_m \mathbf{G}(h) \in \mathcal{L}(\mathbb{R}^{d_e}; \mathbb{R}^{|\mathcal{V}|}) \cong \mathbb{R}^{|\mathcal{V}| \times d_e}$. For any function $\mathbf{H} : \mathbb{R}^{d_e \times |\mathcal{V}|} \rightarrow R_{\mathbf{H}}$, where $R_{\mathbf{H}}$ denotes the range of \mathbf{H} , define $D^{(e)} \mathbf{H}(\varphi) = \partial_{\varphi} \mathbf{H}(\varphi) \in \mathcal{L}(\mathbb{R}^{d_e \times |\mathcal{V}|}, R_{\mathbf{H}})$. In particular we define $\mathbf{H} : \mathbb{R}^{d_e \times |\mathcal{V}|} \times \mathcal{F}^M \rightarrow \mathbb{R}^{|\mathcal{V}|}$ by

$$\mathbf{H}(\varphi, f) := \mathbf{G}(\phi \circ f).$$

This abstract construction mimics the dependence of \mathbf{q}_m on ϕ , and hence on φ . Define also $D^{(e)} \mathbf{H}(\varphi, f) = \partial_{\varphi} \mathbf{H}(\varphi, f)$. For every $(\varphi, f) \in \mathbb{R}^{d_e \times |\mathcal{V}|} \times \mathcal{F}^M$ we have $D^{(e)} \mathbf{H}(\varphi, f) \in \mathcal{L}(\mathbb{R}^{d_e \times |\mathcal{V}|}, \mathbb{R}^{|\mathcal{V}|}) \cong \mathbb{R}^{|\mathcal{V}| \times |\mathcal{V}| d_e}$.

Lemma A.1. *Viewing $D_m \mathbf{G}(h)$ as an element in $\mathbb{R}^{|\mathcal{V}| \times d_e}$ and viewing $D^{(e)} \mathbf{H}(\varphi, f)$ as an element in $\mathbb{R}^{|\mathcal{V}| \times |\mathcal{V}| d_e}$, we obtain*

$$D^{(e)} \mathbf{H}(\varphi, f) = \left(\sum_{m=1}^M D_m \mathbf{G}(\phi \circ f.) \delta_{1, f_m}, \quad \dots, \sum_{m=1}^M D_m \mathbf{G}(\phi \circ f.) \delta_{|\mathcal{V}|, f_m} \right).$$

Proof. Let $h = \phi \circ f$. Note that $\sum_{m=1}^M D_m \mathbf{G}(h) \delta_{k, f_m}$ appearing in the k^{th} position in the preceding identity is an element in $\mathbb{R}^{|\mathcal{V}| \times d_e}$. Since there are $|\mathcal{V}|$ such matrices stacked in a row we see that the preceding identity is indeed an element in $\mathbb{R}^{|\mathcal{V}| \times |\mathcal{V}| d_e}$ as required. Since $\phi(v) = \theta_v$ and $h_m = \phi(f_m)$,

$$D^{(e)} h_m = (\partial_{\theta_1} h_m, \quad \dots, \partial_{\theta_{|\mathcal{V}|}} h_m) = (\delta_{1, f_m} I, \quad \dots, \delta_{|\mathcal{V}|, f_m} I).$$

By the chain rule,

$$D^{(e)} \mathbf{G}(h_1, \dots, h_M) = \sum_{m=1}^M D_m \mathbf{G}(h_1, \dots, h_M) D^{(e)} h_m.$$

From a linear algebra perspective, we have the sum of products of matrices with sizes $\mathbb{R}^{|\mathcal{V}| \times d_e}$ and $\mathbb{R}^{d_e \times d_e |\mathcal{V}|}$, resulting in a matrix of size $\mathbb{R}^{|\mathcal{V}| \times d_e |\mathcal{V}|}$ with the desired form. \square

We may now use the preceding lemma with $\mathbf{G}(h_{1:\ell-1}) = \mathbf{q}_{1:\ell}(\cdot | h_{1:\ell-1}; \vartheta)$ and $h = \phi \circ f$ to compute the derivative of \mathbf{q}_m with respect to φ .

A.2. ϑ Derivative

Here we discuss evaluation of the derivatives of the next-token probability model (5.1) with respect to the model parameters ϑ : the parameters defining the linear transformation \mathbf{B} and the set transformer \mathbf{T} in Subsection 5.2. Recall that the conditional probabilities needed to define the model take the form

$$\mathbf{q}_{1:\ell}(\cdot | h_{1:\ell-1}; \vartheta) = \sigma(\mathbf{B} \circ \mathbf{T}(h_{1:\ell-1}) / \tau).$$

where we may write $\vartheta = (\theta^{(b)}, \theta^{(t)})$ and $\theta^{(b)}$ (resp. $\theta^{(t)}$) are the parameters entering \mathbf{B} (resp. \mathbf{T} .) We recall that $\mathbf{B} \in \mathcal{L}(\mathbb{R}^{d_e}; \mathbb{R}^{|V|}) \cong \mathbb{R}^{|V| \times d_e}$ and we may simply view $\theta^{(b)}$ as an element of $\mathbb{R}^{|V| \times d_e} \equiv \mathbb{R}^{d_b}$, with $d_b = |V|d_e$ (although learning parameterization of \mathbf{B} in lower dimension is also possible.) We have thus identified \mathbf{B} with $\theta^{(b)}$ and its derivatives with respect to $\theta^{(b)}$ is simply the identity map. The parameterization of \mathbf{T} is through the parameters of each attention map \mathbf{A}_k appearing in (5.6), and lies in a Euclidean space isomorphic to \mathbb{R}^{d_T} . The derivative of \mathbf{T} with respect to $\theta^{(t)}$ is thus an element of $\mathcal{L}(\mathbb{R}^{d_T}; \mathbb{R}^{d_e})$. We also note that $\sigma(z): \mathbb{R}^{|V|} \rightarrow \mathbb{R}^{|V|}$ and $\sigma'(z) \in \mathcal{L}(\mathbb{R}^{|V|}; \mathbb{R}^{|V|}) \cong \mathbb{R}^{|V| \times |V|}$. Combining these derivatives we may use the chain rule to compute derivatives of $\mathbf{q}_m(\cdot | h_{1:\ell-1}; \vartheta)$ with respect to ϑ .

Appendix B: Probabilistic Perspective on the Set Transformer Architecture

In this section, we interpret the set transformer architecture described in Section 5 through attention maps acting on probability measures on \mathbb{R}^{d_e} , rather than on sequences of arbitrary length in \mathbb{R}^{d_e} . This perspective is useful for applications of the set transformer outside LLMs. It is also useful for the interpretation of LLMs and how text sequences are represented.

Encoding Sequences as Empirical Measures. The first step in this interpretation of the set transformer is to encode sequences in a manner that is independent of their length. To this end, we define an encoding operator

$$\mathsf{E} : \bigcup_{\ell=1}^L \mathsf{F}_e^\ell \rightarrow \mathcal{P}(\mathbb{R}^{d_e}), \quad \mathsf{E} h_{1:\ell} = \frac{1}{\ell} \sum_{k=1}^{\ell} \delta_{h_k}. \quad (\text{B.1})$$

Now recall the notation for a sequence $h_{1:m-1} := (h_1, \dots, h_{m-1}) \in \mathsf{F}_e^{(m-1)}$. We process this sequence to obtain a probability measure in \mathbb{R}^{d_e} using the empirical measure

$$p^{(m-1)} := \mathsf{E} h_{1:m-1} = \frac{1}{(m-1)} \sum_{k=1}^{m-1} \delta_{h_k}. \quad (\text{B.2})$$

Set Transformer Acting on Probability Measures. The architecture is composed of parameterized *attention* maps $\mathcal{A}_k: \mathcal{P}(\mathbb{R}^{d_e}) \rightarrow \mathcal{P}(\mathbb{R}^{d_e})$, seen as acting between spaces of probability measures, and a pooling layer $\mathfrak{P}: \mathcal{P}(\mathbb{R}^{d_e}) \rightarrow \mathbb{R}^{d_e}$, seen as mapping probability measures into Euclidean space. In particular, the set transformer $\mathbf{T}: \mathsf{F}_e^{(m-1)} \rightarrow \mathbb{R}^{d_e}$ is defined by

$$\mathbf{T}(h_{1:m-1}) = \mathfrak{P} \circ \mathcal{A}_K \circ \dots \mathcal{A}_1(p^{(m-1)}), \quad (\text{B.3})$$

where $p^{(m-1)} = \mathsf{E} h_{1:m-1}$ is defined by (B.2). We describe the attention \mathcal{A}_k and pooling \mathfrak{P} components of the transformer next.

Attention Maps. Given a probability density⁷ $p \in \mathcal{P}(\mathbb{R}^{d_e})$, we define the map $\mathcal{A}(p) = \mathfrak{A}(\cdot; p) \sharp p$ by the pushforward of a transport map $\mathfrak{A}(\cdot; p): \mathbb{R}^{d_e} \rightarrow \mathbb{R}^{d_e}$. To define the transport, we need the following definition of the s -parameterized density $\pi(\cdot; s)$ found by reweighting p :

$$\begin{aligned} \pi(u; s) &= \frac{1}{Z(s)} \exp(\langle Qs, Ku \rangle_{\mathbb{R}^c}) p(u), \\ Z(s) &= \int_{\mathbb{R}^{d_e}} \exp(\langle Qs, Ku \rangle_{\mathbb{R}^c}) p(u) du. \end{aligned}$$

⁷We allow empirical measures to be included in this definition of “density”

The map \mathfrak{A} is then defined by the following sequence of operations:

$$\mathfrak{A}(s; p) \leftarrow s + V \mathbb{E}_{u \sim \pi(\cdot; s)}[u], \quad u \in \mathbb{R}^{d_e}, \quad (\text{B.4a})$$

$$\mathfrak{A}(s; p) \leftarrow \mathfrak{N}(\mathfrak{A}(s; p); \mathfrak{A}(\cdot; p) \sharp p), \quad (\text{B.4b})$$

$$\mathfrak{A}(s; p) \leftarrow s + \mathfrak{NM}(\mathfrak{A}(s; p)), \quad (\text{B.4c})$$

$$\mathfrak{A}(s; p) \leftarrow \mathfrak{N}(\mathfrak{A}(s; p); \mathfrak{A}(\cdot; p) \sharp p), \quad (\text{B.4d})$$

where $\mathfrak{N} : \mathbb{R}^{d_e} \times \mathcal{P}_e^{(m-1)} \rightarrow \mathcal{F}_e^{(m-1)}$ and $\mathfrak{NM} : \mathbb{R}^{d_e} \rightarrow \mathbb{R}^{d_e}$ denote normalization and neural network maps, respectively. These maps are defined in Section 5.1 as acting elementwise, which here we extend to also depend on an input measure for the normalization map. Example B.1 provide an example of a normalization map that also depends on a probability distribution.

We have defined \mathfrak{A} as acting on general probability densities, and note that the definition is readily interpreted to include action on empirical measures $p = p^{(m-1)}$. In particular, when the map \mathfrak{A} is both parameterized by an empirical measure and it is evaluated at each element in the empirical measure, i.e., $h_k \leftarrow \mathfrak{A}(h_k; p^{(m-1)})$ for $k = 1, \dots, m-1$ and the four steps in (B.4), we arrive at the definition of the attention block as acting on sequences in (5.3).

Example B.1 (Batch Normalization). *This normalization depends on input measure π on \mathbb{R}^{d_e} . It is defined by computing the mean and variance of π and applying the operation*

$$\mathfrak{N}(u; \pi) = D \frac{(u - \mathbb{E}_{u \sim \pi}[u]))}{\sqrt{\mathbb{V}_{u \sim \pi}[u]} + \varepsilon} + b,$$

where $D \in \mathbb{R}^{d_e \times d_e}$ and $b \in \mathbb{R}^{d_e}$ are trainable parameters as in Example 5.2; $\varepsilon > 0$ is a user-prescribed stabilization constant.

This normalization is typically applied when evaluating the attention map on a batch of input sequences $h^{(1)}, \dots, h^{(N)}$ where each sequence $h^{(n)} = (h_1^{(n)}, \dots, h_\ell^{(n)})$ for a given length ℓ . By assuming the sequence elements and batches are independent, π can be defined as the empirical measure

$$\pi = \frac{1}{\ell n} \sum_{k=1}^{\ell} \sum_{n=1}^N \delta_{h_k^{(n)}}.$$

By using larger batch sizes, we can expect to learn parameters that generalize well to input measures that are representative of the population-level limit over sequences defined in Data Assumption 4.1.

Pooling Operator The operator $\mathfrak{P} : \mathcal{P}(\mathbb{R}^{d_e}) \rightarrow \mathbb{R}^{d_e}$ is a function acting on probability measures and returning a vector. This function includes the case of linear functionals on measures, written for $\mathfrak{f} : \mathbb{R}^{d_e} \mapsto \mathbb{R}^{d_e}$, as

$$\mathfrak{P}(p) = \int \mathfrak{f}(h) dp(h). \quad (\text{B.5})$$

In the context of the set transformer, \mathfrak{P} is defined so that, when it acts on an empirical measure defined from a sequence as in (B.1), the overall mapping is both permutation-invariant and is well-defined for input sequences of arbitrary length. The following example contains the population-level variant of the widely used choices defined in Example 5.4 that satisfy these properties.

Example B.2. *The mean pooling operation is given by choosing $\mathfrak{f}(h) = h$, which yields the operator*

$$\mathfrak{P}(p) = \int h dp(h).$$

The max pooling operation is defined by choosing the elementwise operation $\mathfrak{f}(h)_j = \max((h)_j)$ for each $h \in \mathbb{R}^{d_e}$ and $j = 1, \dots, d_e$. The continuum analog underlying max pooling is to choose to compute the elementwise essential supremum, which can be defined as a limit:

$$\mathfrak{P}(p)_j = \lim_{\beta \rightarrow \infty} \frac{1}{\beta} \log \left(\int e^{\beta(h)_j} p(h) dh \right).$$

Appendix C: Continuum State-Space Models

In this section we provide a continuous time perspective on the state-space models introduced in Subsection 5.3.4. We view the state-space models as time-discretizations defined through a continuously evolving hidden state, driven by a continuous-in-time input.

Structured State Space Models (SSMs) map an input $h: [0, T] \rightarrow \mathbb{R}^{d_e}$ into output $u: [0, T] \rightarrow \mathbb{R}^{d_e}$. This is achieved by evolving a hidden state $v(t) \in \mathbb{R}^s$ that takes h as input in a causal way, and then defining the output u through a function, that takes both v and h as input, acting pointwise in time. The model is parameterized by $\vartheta = (\vartheta_0, \vartheta_1, \vartheta_2)$ and takes the form

$$\frac{dv}{dt} = \mathcal{F}(v, h; \vartheta_1), \quad v(0) = \vartheta_0, \quad (\text{C.1a})$$

$$u = \mathcal{G}(v, h; \vartheta_2); \quad (\text{C.1b})$$

here the operators $\mathcal{F}(\cdot, \cdot; \vartheta_1): \mathbb{R}^s \times \mathbb{R}^{d_e} \rightarrow \mathbb{R}^s$ and $\mathcal{G}(\cdot, \cdot; \vartheta_2): \mathbb{R}^s \times \mathbb{R}^{d_e} \rightarrow \mathbb{R}^{d_e}$ define the evolution of the state and the output starting from the initial condition $\vartheta_0 \in \mathbb{R}^s$. One natural choice is to define operators via the affine structure

$$\mathcal{F}(v, h; \vartheta) = Av + Bh, \quad (\text{C.2a})$$

$$\mathcal{G}(v, h; \vartheta) = Cv + Dh, \quad (\text{C.2b})$$

so that ϑ is defined by the matrices $A \in \mathbb{R}^{s \times s}$, $B \in \mathbb{R}^{s \times d_e}$, $C \in \mathbb{R}^{d_e \times s}$, $D \in \mathbb{R}^{d_e \times d_e}$. That is, the model parameters are given by $\vartheta = (\vartheta_0, A, B, C, D)$. The dimensionality of the hidden state is commonly chosen to be (considerably) larger than the embedding dimension of the sequence elements: $s \gg d_e$.

Solving (C.1), under (C.2), yields

$$v(t) = e^{At} \vartheta_0 + \int_0^t e^{At} B e^{-As} h(s) ds, \quad (\text{C.3a})$$

$$u(t) = Cv(t) + Dh(t), \quad (\text{C.3b})$$

which defines a map from an input h to the output u .

Remark C.1. This map, discretized in time, can be used in place of the attention mechanism in (B.4a). In practice, the input sequence is represented at discrete-times $t_k \in [0, T]$ by considering a step-size $\Delta t \geq 0$. The evolution of the hidden state $v_k := v(t_k)$ for the linear system as a function of $(h_k)_{k=1}^N$ and $h_k := h(t_k)$ is then given by the discrete-time equations

$$v_{k+1} = e^{A\Delta t} v_k + e^{A t_{k+1}} \left(\int_0^{\Delta t} B e^{-Az} dz \right) e^{-A t_k} h_k, \quad (\text{C.4a})$$

$$u_{k+1} = Cv_{k+1} + Dh_{k+1}. \quad (\text{C.4b})$$

Appendix D: Proof of Reversibility of Discrete Diffusion

Recall $\mathbf{p}(\cdot, t)$ solving (9.1) and $\bar{\mathbf{p}}(\cdot, t)$ solving (9.4). We have the following theorem concerning their relationship to one another:

Theorem D.1. *Let $f(\cdot) : [0, T] \rightarrow \mathcal{V}$ be a sequence that follows a CTMC according to the rate matrix $Q(t) \in \mathbb{R}^{|\mathcal{V}| \times |\mathcal{V}|}$ and has marginal probability $\mathbf{p} : \mathcal{V} \times [0, T] \rightarrow \mathcal{P}(\mathcal{V})$. Now consider a sequence $\bar{f}(\cdot)$ evolving in reverse-time that follows a CTMC according to the rate matrix $\bar{Q}(t)$ with entries*

$$\bar{Q}_{ij}(t) = Q_{ji}(t) \frac{\mathbf{p}(j, t)}{\mathbf{p}(i, t)}, \quad (\text{D.1})$$

for all $t \in [0, T]$ and $1 \leq i, j \leq |\mathcal{V}|$. Let $\bar{f}(t)$ have marginal probability $\bar{\mathbf{p}}(\cdot, t) : \mathcal{V} \times [0, T] \rightarrow \mathcal{P}(\mathcal{V})$ and run the process backwards on $[0, T]$, starting from $\bar{f}(T) \sim \mathbf{p}(\cdot, T)$. Then, $\bar{f}(t) \stackrel{d}{=} f(t) : \bar{\mathbf{p}}(\cdot, t) = \mathbf{p}(\cdot, t)$ for all $t \in [0, T]$.

Proof. If \bar{f} is a CTMC, then its marginal probability $\bar{\mathbf{p}}$ evolves according to the forward equation:

$$\begin{aligned} \frac{d\bar{\mathbf{p}}(i, t)}{dt} &= \sum_{k \in \mathcal{V}} \bar{Q}_{ki}(t) \bar{\mathbf{p}}(k, t) \\ &= \sum_{k \neq i} \bar{Q}_{ki}(t) \bar{\mathbf{p}}(k, t) + \bar{Q}_{ii}(t) \bar{\mathbf{p}}(i, t) \\ &= \sum_{k \neq i} \bar{Q}_{ki}(t) \bar{\mathbf{p}}(k, t) + \left(- \sum_{\ell \neq i} \bar{Q}_{i\ell}(t) \right) \bar{\mathbf{p}}(i, t), \end{aligned}$$

where in the last line we used the row-sum property for the rate matrix $\sum_{\ell} \bar{Q}_{i\ell}(t) = 0$ for all i . Using the definition for the reverse rate matrix in (D.1) we have

$$\frac{d\bar{\mathbf{p}}(i, t)}{dt} = \sum_{k \neq i} Q_{ik}(t) \frac{\mathbf{p}(i, t)}{\mathbf{p}(k, t)} \bar{\mathbf{p}}(k, t) - \sum_{\ell \neq i} Q_{\ell i}(t) \frac{\mathbf{p}(\ell, t)}{\mathbf{p}(i, t)} \bar{\mathbf{p}}(i, t).$$

Observe that taking $\bar{\mathbf{p}}(k, t) = \mathbf{p}(k, t)$ for all $k = 1, \dots, |\mathcal{V}|$, then we have

$$\begin{aligned} \frac{d\mathbf{p}(i, t)}{dt} &= \frac{d\bar{\mathbf{p}}(i, t)}{dt} = \sum_{k \neq i} Q_{ik}(t) \mathbf{p}(i, t) - \sum_{\ell \neq i} Q_{\ell i}(t) \mathbf{p}(\ell, t) \\ &= (-Q_{ii}(t)) \mathbf{p}(i, t) - \sum_{\ell \neq i} Q_{\ell i}(t) \mathbf{p}(\ell, t) \\ &= - \sum_{\ell \neq i} Q_{\ell i}(t) \mathbf{p}(\ell, t), \end{aligned}$$

which is the forward equation for the marginal probability \mathbf{p} after accounting for the change in the sign for the drift from evolving the equation backwards-in-time. By uniqueness of $\mathbf{p}(\cdot, t)$ solving (9.1) and $\bar{\mathbf{p}}(\cdot, t)$ solving (9.4) the result follows. \square

Appendix E: Details of Prompts and Answers

E.1. Question Answering

The following example supplements the discussion in Subsection 7.1.

"prompt": A man named Frank travels from NYC to Philadelphia by road, on a Monday, leaving at 9:00am and arriving at 12noon. He then travels from Philadelphia to NYC the next day, Tuesday, also leaving at 9:00am and arriving at 12 noon. He takes the same route, but on Tuesday reverses the route taken on Monday. Is it necessarily the case that there is at least one point that he will be located at the same time, albeit on the two different days? Explain your answer

"output": Yes, it is necessarily the case that there is at least one point where Frank will be located at the same time on both days. This is due to the Intermediate Value Theorem, which states that if a continuous function takes values $f(a)$ and $f(b)$ at points a and b , respectively, then it also takes any value between $f(a)$ and $f(b)$ at some point between a and b .

In this scenario, we can consider Frank's position as a continuous function of time. On Monday, he travels from NYC to Philadelphia, and on Tuesday, he travels from Philadelphia back to NYC. Since he takes the same route on both days, his position as a function of time will be continuous.

Let's denote Frank's position on Monday as $f(t)$ and on Tuesday as $g(t)$, where t represents time. Since Frank arrives at 12 noon on both days, we have $f(12) = g(12)$. Now, let's consider the function $h(t) = f(t) - g(t)$. This function represents the difference in Frank's position between Monday and Tuesday.

Since Frank's position is continuous, $h(t)$ is also continuous. Moreover, $h(9) = f(9) - g(9)$ represents the difference in Frank's position at 9:00am on both days, and $h(12) = f(12) - g(12) = 0$, as Frank arrives at the same time on both days.

By the Intermediate Value Theorem, there must be some time t between 9:00am and 12:00pm where $h(t) = 0$, meaning that Frank's position on Monday and Tuesday is the same at that time. Therefore, it is necessarily the case that there is at least one point where Frank will be located at the same time on both days.<|endoftext|>

E.2. Conversations

The example in this subsection supplements the discussion in Subsection 7.2, on question and answering with LLMs, by extending the example on Bayes' theorem.

"prompt": Now explain it more formally to a mathematician.

"output": Bayes' theorem is a fundamental concept in probability theory that allows us to calculate the conditional probability of an event given prior knowledge of other related events. Mathematically, it is expressed as follows:

$$P(A|B) = (P(B|A) * P(A)) / P(B)$$

Where:

- $P(A|B)$ is the posterior probability of event A occurring given that event B has occurred.
- $P(B|A)$ is the likelihood of event B occurring given that event A has occurred.
- $P(A)$ is the prior probability of event A occurring.
- $P(B)$ is the marginal probability of event B occurring.

In simpler terms, Bayes' theorem helps us update our beliefs or probabilities about an event based on new evidence provided by other related events. It is

```
widely used in various fields such as statistics, machine learning, and
artificial intelligence to make predictions and decisions under
uncertainty.<|endoftext|>
```

E.3. Mathematics

In this subsection we compare the outputs of the LLM, with and without context, for a multiplication task. We consider the multiplication of six different pairs of integers, where each pair contains a two digit and three digit number. Our initial experiments will use deterministic greedy-decoding. We will then compare the responses with those obtained using a stochastic sampling procedure: positive temperature τ is used at inference time; see Remark 6.2.

First, we demonstrate the deterministic algorithm for calculating 473×45 ; the correct answer is 21285. When context is not provided in the prompt, an incorrect answer is given:

```
"prompt": Calculate 473*45
"output": To calculate  $(473 \times 45)$ , we can use the standard
multiplication method:

\[
\begin{array}{r}
473 \\
\times 45 \\
\hline
2365 \quad (\text{This is } 473 \times 5) \\
+ 18920 \quad (\text{This is } 473 \times 40, \text{ shifted one position to the
left}) \\
\hline
21385
\end{array}
\]

So,  $(473 \times 45 = 21385)$ .<|im_end|>
```

However, if we provide context in the prompt, then the correct answer is given. Here, the context comprises the necessary skills, together with an example in which integer multiplication is built-up, step-by-step, using the provided skills.

```
"context": Skill <extract_digits>: Extract the digits in a number to a list.
For example, Extract digits in 123 to D=[1,2,3]. Extract digits in 7654 to
D=[7,6,5,4]. \
Skill <list_length>: Get the number of elements in a list.
For example, D=[1,2,3], len(D)=3. A=[1,2,4,5,6], len(A)=5.

Skill <mul_two_single_digit_number>: Multiply two single-digit numbers.
0*1=0 0*2=0 0*3=0 0*4=0 0*5=0 0*6=0 0*7=0 0*8=0 0*9=0
1*1=1 1*2=2 1*3=3 1*4=4 1*5=5 1*6=6 1*7=7 1*8=8 1*9=9
2*1=2 2*2=4 2*3=6 2*4=8 2*5=10 2*6=12 2*7=14 2*8=16 2*9=18
3*1=3 3*2=6 3*3=9 3*4=12 3*5=15 3*6=18 3*7=21 3*8=24 3*9=27
4*1=4 4*2=8 4*3=12 4*4=16 4*5=20 4*6=24 4*7=28 4*8=32 4*9=36
5*1=5 5*2=10 5*3=15 5*4=20 5*5=25 5*6=30 5*7=35 5*8=40 5*9=45
6*1=6 6*2=12 6*3=18 6*4=24 6*5=30 6*6=36 6*7=42 6*8=48 6*9=54
7*1=7 7*2=14 7*3=21 7*4=28 7*5=35 7*6=42 7*7=49 7*8=56 7*9=63
8*1=8 8*2=16 8*3=24 8*4=32 8*5=40 8*6=48 8*7=56 8*8=64 8*9=72
9*1=9 9*2=18 9*3=27 9*4=36 9*5=45 9*6=54 9*7=63 9*8=72 9*9=81
```

Skill <add_multiple_numbers>: Add multiple numbers such as $m+n+p$:

1. Add the first two numbers $m+n$ and get the result $r_1=m+n$.

2. Add the third number p to r_1 and get the result $r_2=r_1+p$.

For example, calculate $128+64+79$:

1. Add the first two numbers $128+64$ and get the result $r_1=128+64=192$.

2. Add the third number 79 to r_1 and get the result $r_2=192+79=271$.

So $128+64+79=271$.

Example: Calculate $184*67$:

Answer:

1. Using Skill <extract_digits> and Skill <list_length>, extract the digits in 184 to $DM=[1, 8, 4]$.

$\text{len}(DM)=3$. Extract the digits in 67 to $DN=[6, 7]$. $\text{len}(DN)=2$.

2. Add $0, 1, \text{len}(DM)-1=2$ zeros to the end of every number in $DM=[1, 8, 4]$ according to the position of the number in DM : $DMO=[1*100, 8*10, 4*1]=[100, 80, 4]$.

3. Add $0, \text{len}(DN)-1=1$ zeros to the end of every number in $DN=[6, 7]$ according to the position of the number in DN : $DNO=[6*10, 7*1]=[60, 7]$.

4. Using Skill <mul_two_single_digit_number>, multiple every number in $DMO=[100, 80, 4]$

with every number in $DNO=[60, 7]$ and get $R=[100*60, 100*7, 80*60, 80*7, 4*60, 4*7]=[6000, 700, 4800, 560, 240, 28]$.

5. Using Skill <add_multiple_numbers>, add all the numbers in $R=[6000, 700, 4800, 560, 240, 28]$,

$6000+700+4800+560+240+28$:

i. Add the first two numbers: $r_1=6000+700=6700$.

ii. Add the third number 4800 to $r_1=6700$: $r_2=6700+4800=11500$.

iii. Add the fourth number 560 to $r_2=11500$: $r_3=11500+560=12060$.

iv. Add the fifth number 240 to $r_3=12060$: $r_4=12060+240=12300$.

v. Add the sixth number 28 to $r_4=12300$: $r_5=12300+28=12328$.

6. So the answer is 12328

"prompt": Calculate $473*45$

"output": Let's break down the calculation step by step:

1. **Extract Digits and Prepare for Multiplication:**

– Extract digits from 473 : $DM = [4, 7, 3]$. $\text{len}(DM) = 3$.

– Extract digits from 45 : $DN = [4, 5]$. $\text{len}(DN) = 2$.

We need to add zeros to the end of each number in DM and DN to align their positions for multiplication:

– $DMO = [4*100, 7*10, 3*1] = [400, 70, 3]$.

– $DNO = [4*10, 5*1] = [40, 5]$.

2. **Multiply Each Pair of Numbers:**

– Now we multiply each number in DMO with each number in DNO :

– $400 * 40 = 16000$

– $400 * 5 = 2000$

– $70 * 40 = 2800$

– $70 * 5 = 350$

– $3 * 40 = 120$

– $3 * 5 = 15$

So, the result R is: $R = [16000, 2000, 2800, 350, 120, 15]$.

3. **Add All Numbers in Result R :**

– Add the first two numbers: $r_1 = 16000 + 2000 = 18000$.

– Add the third number to r_1 : $r_2 = 18000 + 2800 = 20800$.

– Add the fourth number to r_2 : $r_3 = 20800 + 350 = 21150$.

– Add the fifth number to r_3 : $r_4 = 21150 + 120 = 21270$.

```
- Add the sixth number to r4: r5 = 21270 + 15 = 21285.
```

```
Therefore, the final answer is 21285.<|im_end|>
```

We now repeat the comparison between multiplication, undertaken with and without context, for three other pairs of integers. For conciseness, we only include the final line of the LLM's output without and with in-context learning (ICL). We include the true answer for the task below each prompt. We observe that while the model without ICL only produces a correct solution in one out of three examples, ICL correctly solves all three of the multiplication tasks.

```
"prompt": Calculate 299*89
"truth": 26611
"output (Without ICL)": So, \(\( 299 \times 89 = 26911 \)\).<|im_end|>
"output (With ICL)": Therefore, the final answer is 26611.<|im_end|>
```

```
"prompt": Calculate 378*64
"truth": 24192
"output (Without ICL)": So, \(\( 378 \times 64 = 24072 \)\).<|im_end|>
"output (With ICL)": Therefore, the final answer is 24192.<|im_end|>
```

```
"prompt": Calculate 952*76
"truth": 72352
"output (Without ICL)": \[ 952 \times 76 = 72352 \]<|im_end|>
"output (With ICL)": So the answer is 72352.<|im_end|>
```

The reader might have the impression that use of ICL, then, solves the problem of multiplication accuracy. However, this is not the case as the next example shows: here the model without ICL is correct, but adding context leads to the wrong answer:

```
"prompt": Calculate 874*25
"truth": 21850
"output (Without ICL)": So, \(\( 874 \times 25 = 21850 \)\).<|im_end|>
"output (With ICL)": Therefore, \(\( 874 \times 25 = 6128 \)\).<|im_end|>
```

Lastly, we present model responses with stochasticity, exemplifying the discussion in Remark 6.2. Here we set the temperature parameter $\tau = 0.5$. We recall that the choice $\tau = 0$, deployed in all previous experiments, results in a deterministic output, but that any $\tau > 0$ will result in stochastic output. We present the output of the stochastic algorithm for the calculation of 378×64 ; the correct answer is 24192. We include two outputs below from the stochastic algorithm without ICL to demonstrate when the model does and does not produce the correct answer. We observe that the model does produce the correct answer when it uses a reasoning process in the first output.

```
"prompt": Calculate 378*64
"output": To calculate \(\( 378 \times 64 \)\), we can use the standard
multiplication method or a calculator for an exact result.
```

Using the standard multiplication method:

```
\[
\begin{array}{r}
378 \\
\times 64 \\
\hline
\end{array}
```

```

\times 64 \\
\hline
 1512 \quad (\text{378} \times 4) \\
22680 \quad (\text{378} \times 60, \text{shift one position to the left}) \\
\hline
 24192 \\
\end{array}
\]

So, \(( 378 \times 64 = 24192 \)).<|im_end|>

```

```

"prompt": Calculate 378*64
"output": To calculate \(( 378 \times 64 \)), we can use the standard
multiplication method or a calculator for an exact result.

```

Using a calculator, the result is:

```
\[ 378 \times 64 = 24048 \].<|im_end|>
```

To further probe the role of stochastic next-token prediction we compute the output five times with and without ICL. We observe that the model returns the correct answer in four out of five instances without ICL, and in all five instances with ICL.

E.4. Coding

In this example, we present the output from requesting MATLAB code to numerically solve an ODE, contrasting model response with and without fine tuning. Following the code, we include the plot produced by MATLAB for the code resulting from both models. We start without fine-tuning:

```

"prompt": Write {\sc{Matlab}} code to numerically solve a nonlinear ODE with
vector field f. Only include the code in the response.
"output": Sure, here's an example of how you can use the 'ode45' solver in
{\sc{Matlab}} to numerically solve a nonlinear ordinary differential equation
(ODE) with a given vector field 'f':
```\sc{Matlab}
f = @(t, y) [y(2); -y(1) - y(2)^2];
y0 = [1; 0];
tspan = [0 10];
[t, y] = ode45(f, tspan, y0);
plot(t, y(:, 1), 'b', t, y(:, 2), 'r');
xlabel('Time');
ylabel('Solution');
legend('y1', 'y2');
title('Solution of the ODE');
```

```

This code defines the vector field 'f' as a function of time 't' and the state vector 'y'. It then uses the 'ode45' solver to find the solution over the specified time span '[0 10]' with initial conditions 'y0 = [1; 0]'. Finally, it plots the solutions for 'y1' and 'y2' over time.<|endoftext|>

With fine-tuning we obtain a different example:

```


"prompt": Write {\sc{Matlab}} code to numerically solve a nonlinear ODE with
vector field f. Provide only the code for solving.
"output": Sure, here's the code to numerically solve a nonlinear ODE with vector
field f using the 'ode45' solver in {\sc{Matlab}}:



```

```{\sc{Matlab}}
function df = myVectorField(t, y)
    df = [-y + sin(t)];
end

y0 = [1]; %
tspan = [0 10]; %

[t, y] = ode45(@myVectorField, tspan, y0);

plot(t, y);
xlabel('Time (t)');
ylabel('y(t)');
title('Solution of the ODE');
grid on;
```

```


```

This code defines a vector field function 'myVectorField' that represents the right-hand side of your ODE. The 'ode45' function is used to solve the ODE numerically over the specified time span with the given initial conditions. Finally, the solution is plotted using 'plot'. Adjust the vector field function and initial conditions according to your specific problem.<|endoftext|>

The following figure demonstrates the fact that the Qwen based code generator *without* fine-tuning delivers a piece of MATLAB software which integrates an ODE that blows up on the domain of integration; this is clearly undesirable. *With* fine-tuning this issue is not present.

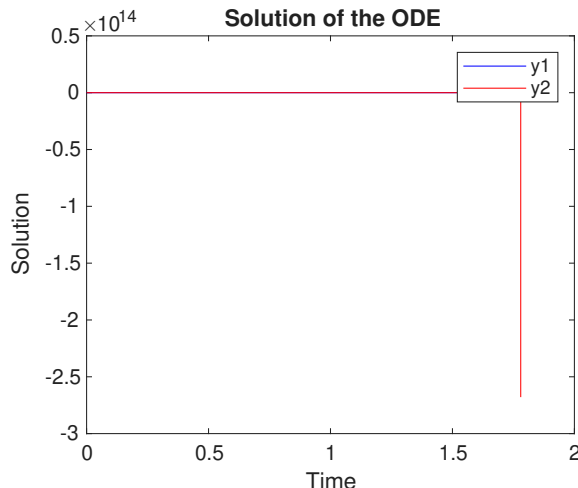


Fig 1: MATLAB output without fine-tuned model: Qwen-2.5 showing a solution which blows-up.

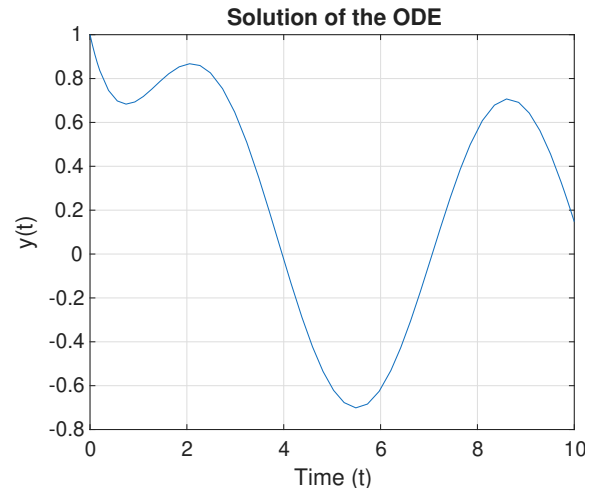


Fig 2: MATLAB output with fine-tuned model: Qwen-2.5-Coder showing a bounded solution.